The 3rd International Workshop on Physics at High Baryon Density (PHD2026)

Mean transverse momentum fluctuations: probing nuclear structure and QCD matter

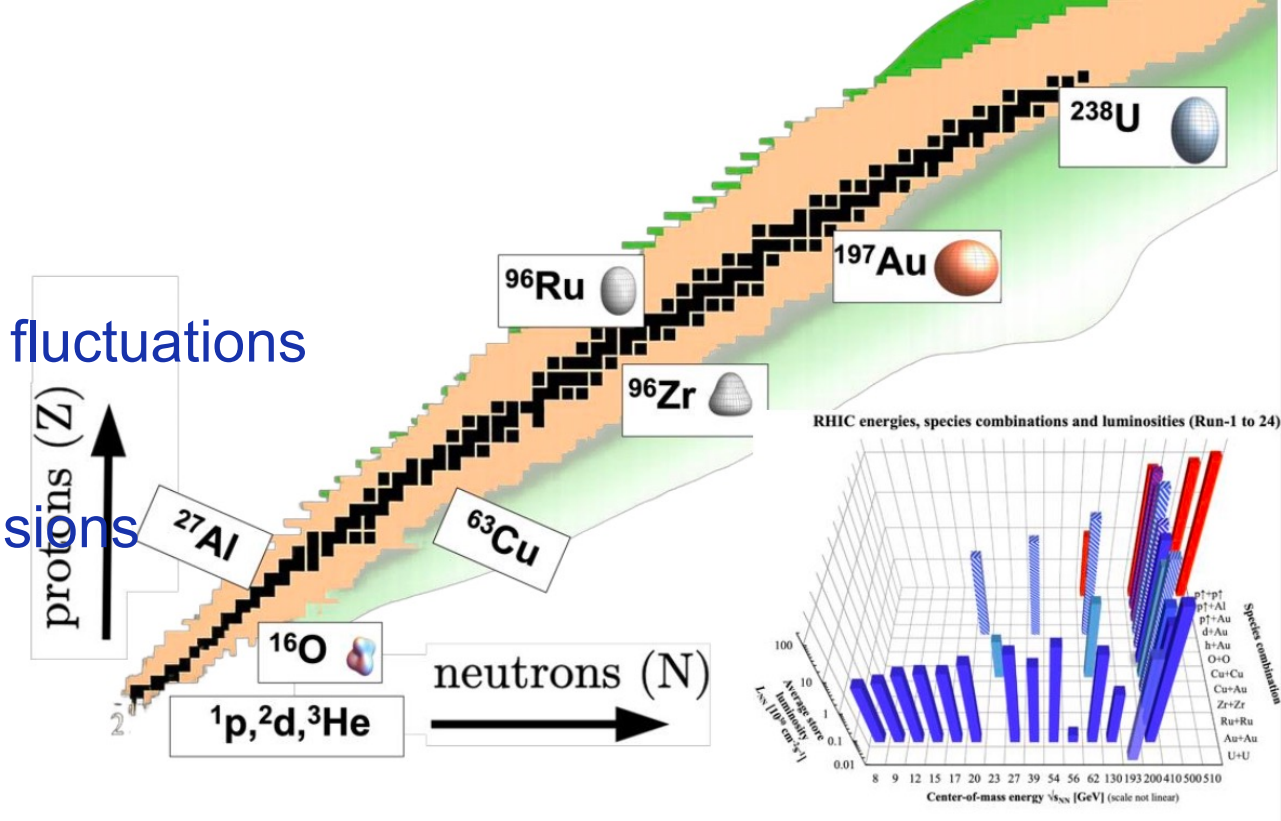
Chunjian Zhang

Fudan University

Dalian, November 13, 2026

Outline

- **Introductions:** mean transverse momentum fluctuations
- Imaging nuclear structure in high-energy collisions
  - I. Nuclear structure in ^{238}U, ^{96}Ru/^{96}Zr
  - II. Geometry effect and subnucleon fluctuations in ^{16}O
- Probing QCD matter properties
  - I. Second-order p_T fluctuation in ^{197}Au + ^{197}Au collisions at FXT energies
  - II. Energy dependence of high-order p_T fluctuations



❑ **Introductions:** mean transverse momentum fluctuations

Imaging by smashing method and event-by-event fluctuations

Take a snapshot

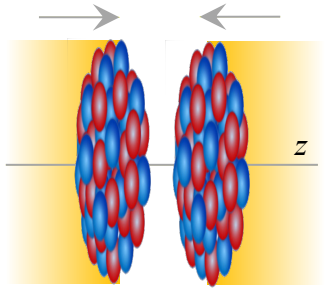
Evolution

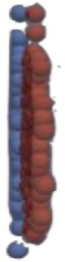
Measurement

Nuclei collisions $T_{\mu\nu}(\tau = 0)$

$\partial_\mu T^{\mu\nu} = 0$, EOS, viscosity…

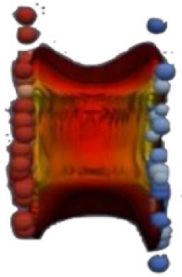
$T_{\mu\nu}(\tau = \infty)$



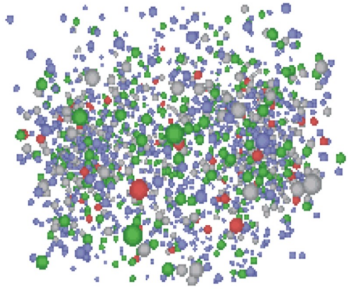


Pressure-driven expansion of

Quark-gluon plasma (QGP)



free-streaming



$\tau \sim 2R_0/\Gamma \sim 0.1\mathrm{fm}/c$
exposure

$\tau \sim 10\mathrm{fm}/c$
expansion

$\tau \sim 10^{15}\mathrm{fm}/c$
detection

J. Jia et al., *Nucl. Sci. Tech. 35, 220 (2024)*

$$\rho(r,\theta,\phi) = \frac{\rho_0}{1 + e^{(r - R(\theta,\phi))/a_0}}$$

- β_2 → quadrupole deformation
- β_3 → octupole deformation
- γ → triaxiality
- a_0 → surface diffuseness
- R_0 → nuclear size

ab initio theory/shell model/DFT

Imaging by smashing method and event-by-event fluctuations

Take a snapshot

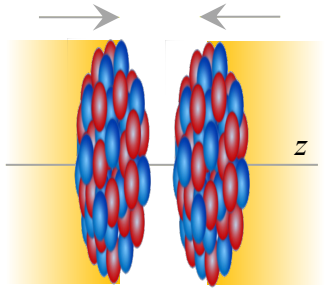
Evolution

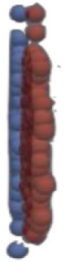
Measurement

Nuclei collisions $T_{\mu\nu}(\tau = 0)$

$\partial_\mu T^{\mu\nu} = 0$, EOS, viscosity…

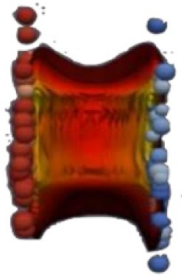
$T_{\mu\nu}(\tau = \infty)$



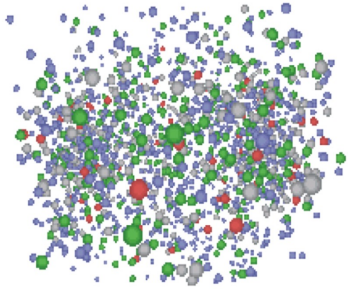


Pressure-driven expansion of

Quark-gluon plasma (QGP)



free-streaming



$\tau \sim 2R_0/\Gamma \sim 0.1\text{fm}/c$

exposure

$\tau \sim 10\text{fm}/c$

expansion

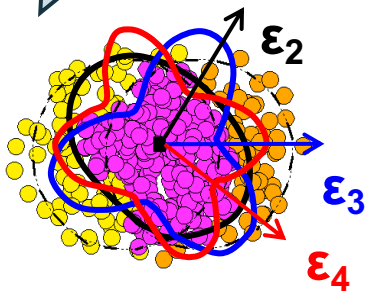
$\tau \sim 10^{15}\text{fm}/c$

detection

$$\rho(r,\theta,\phi) = \frac{\rho_0}{1 + e^{(r - R(\theta,\phi))/a_0}}$$

- β_2 → quadrupole deformation
- β_3 → octupole deformation
- γ → triaxiality
- a_0 → surface diffuseness
- R_0 → nuclear size

ab initio theory/shell model/DFT



size & shape

J. Jia et al., *Nucl. Sci. Tech. 35, 220 (2024)*

$R_\perp^2 \propto \langle r_\perp^2 \rangle$

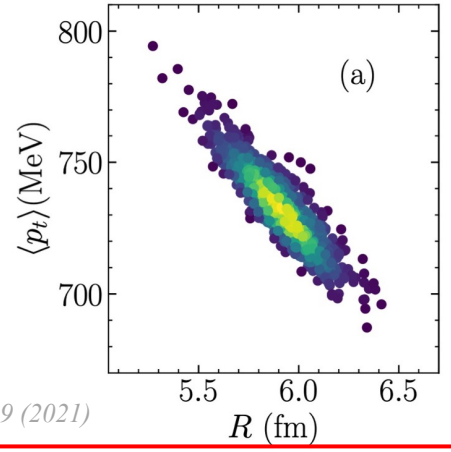
$\mathcal{E}_n \propto \langle r_\perp^n e^{in\phi} \rangle$

R_0 a_0 β_n

Observables $\frac{d^2N}{d\phi dp_T} = N(p_T)\left(\sum_n V_n e^{-in\phi}\right)$

linear responses:

$$\frac{\delta[p_T]}{[p_T]} \propto -\frac{\delta R_\perp}{R_\perp}$$

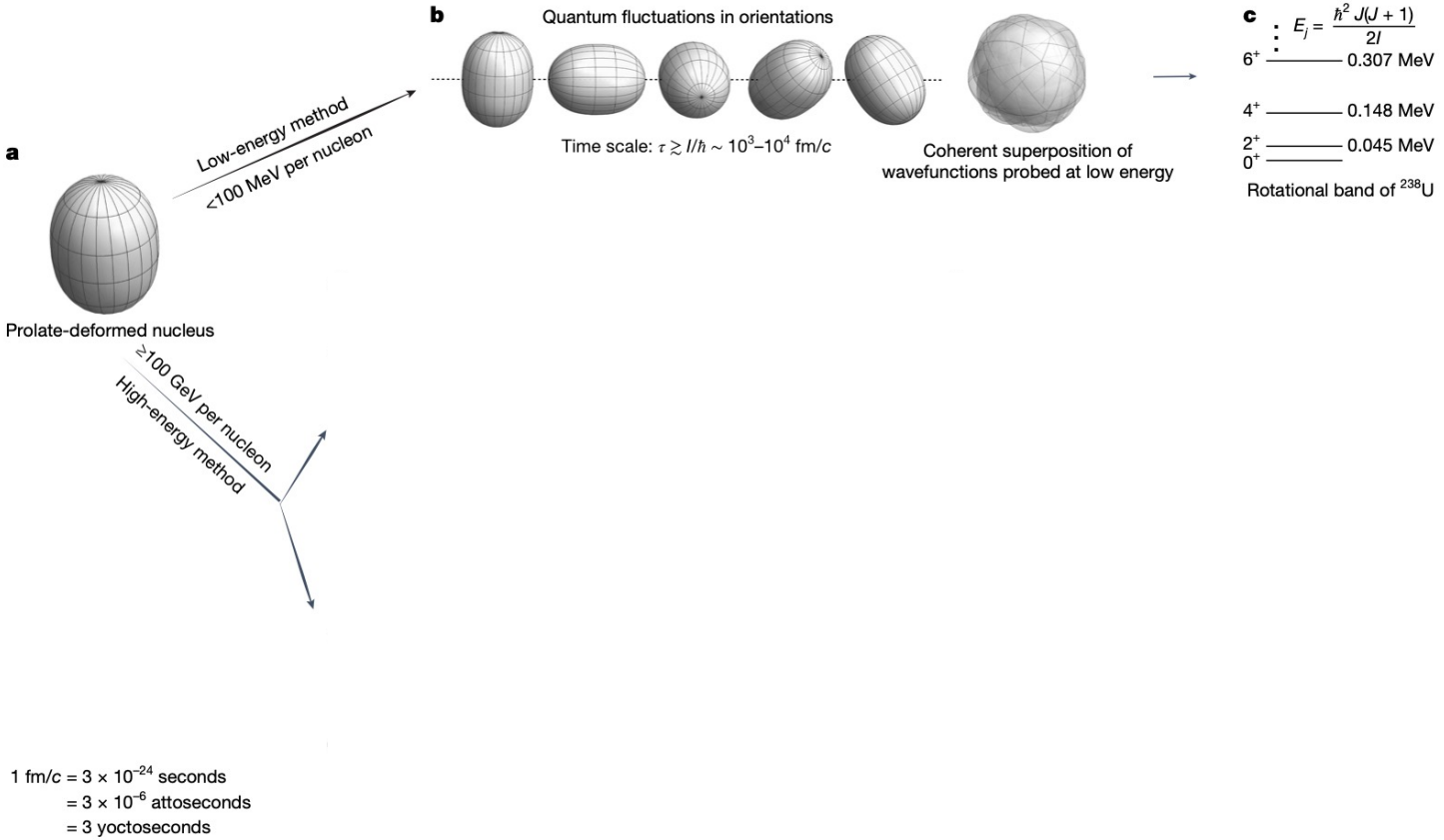


G. Giacalone et al., *PRC 103, 024909 (2021)*

Key: 1) fast snapshot, 2) linear response, 3) large multiplicity for many-body correlation

Imaging nuclear shape in high-energy snapshot

- Nuclear shape in intrinsic (body-fixed) frame not directly visible in the lab frame
  --Mainly inferred from non-invasive spectroscopy methods.



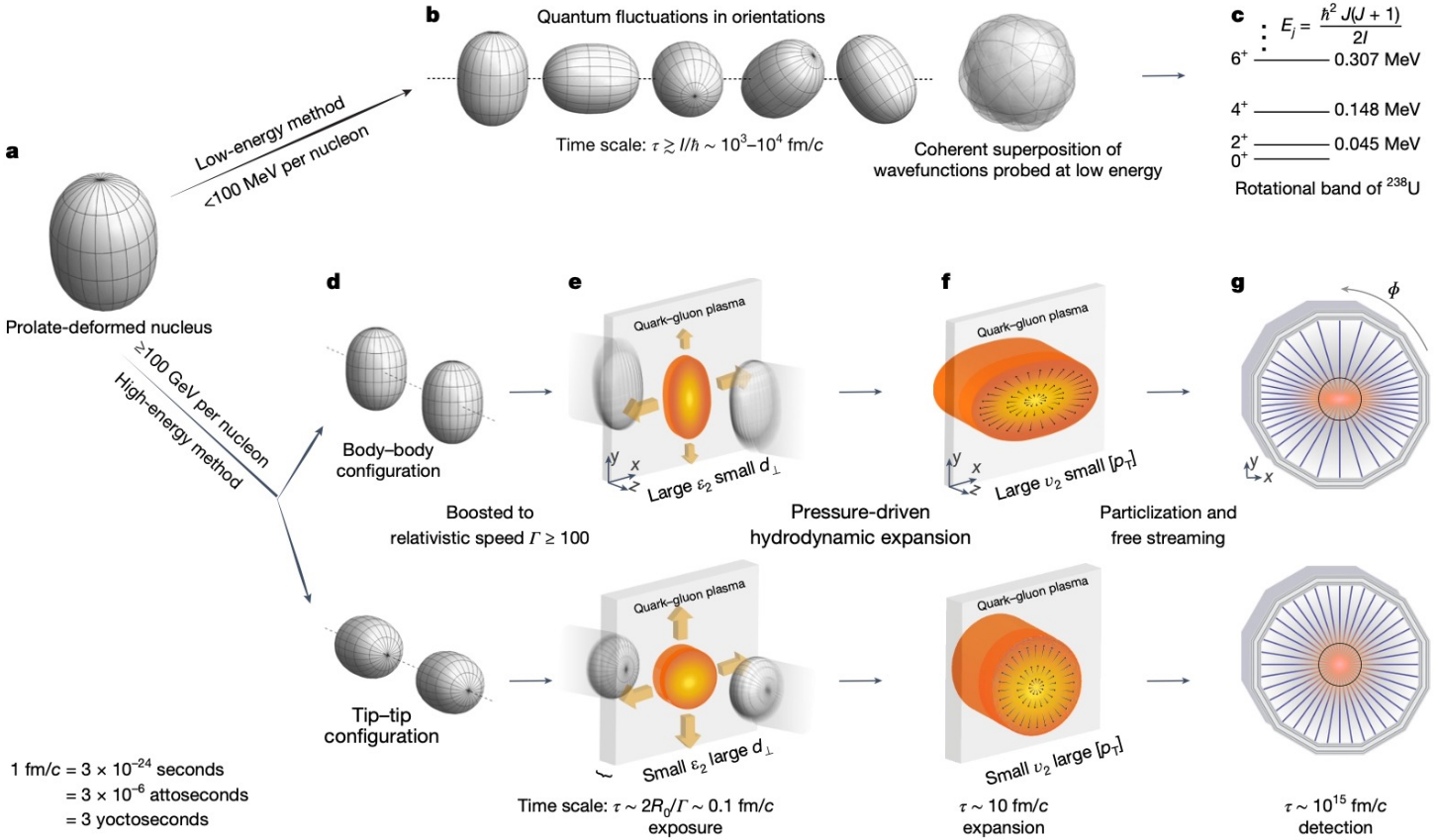
1 fm/c = 3×10^{-24} seconds
= 3×10^{-6} attoseconds
= 3 yoctoseconds

Nuclear deformation across energy scales

STAR, *Nature 635, 67-72 (2024)*
Nature News&Views, Nature News, Nature Podcast

Imaging nuclear shape in high-energy snapshot

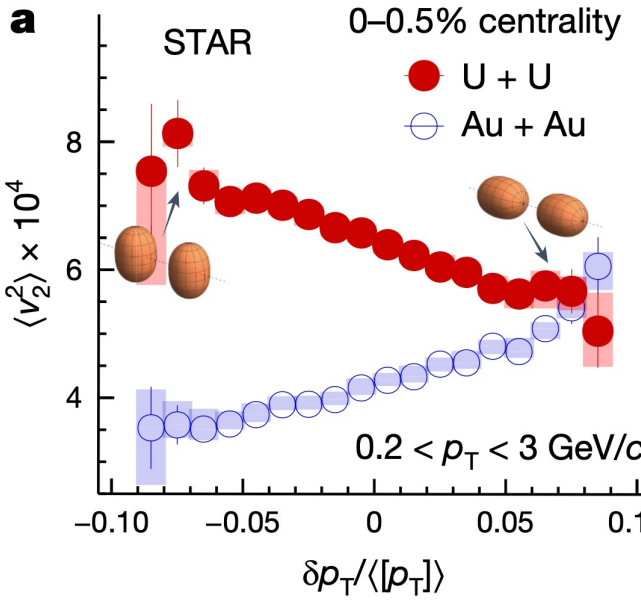
- Nuclear shape in intrinsic (body-fixed) frame not directly visible in the lab frame
  --Mainly inferred from non-invasive spectroscopy methods.



Nuclear deformation across energy scales

STAR, *Nature 635, 67-72 (2024)*
Nature News&Views, Nature News, Nature Podcast

Body-body: $v_2 \nearrow$ $p_T \searrow$

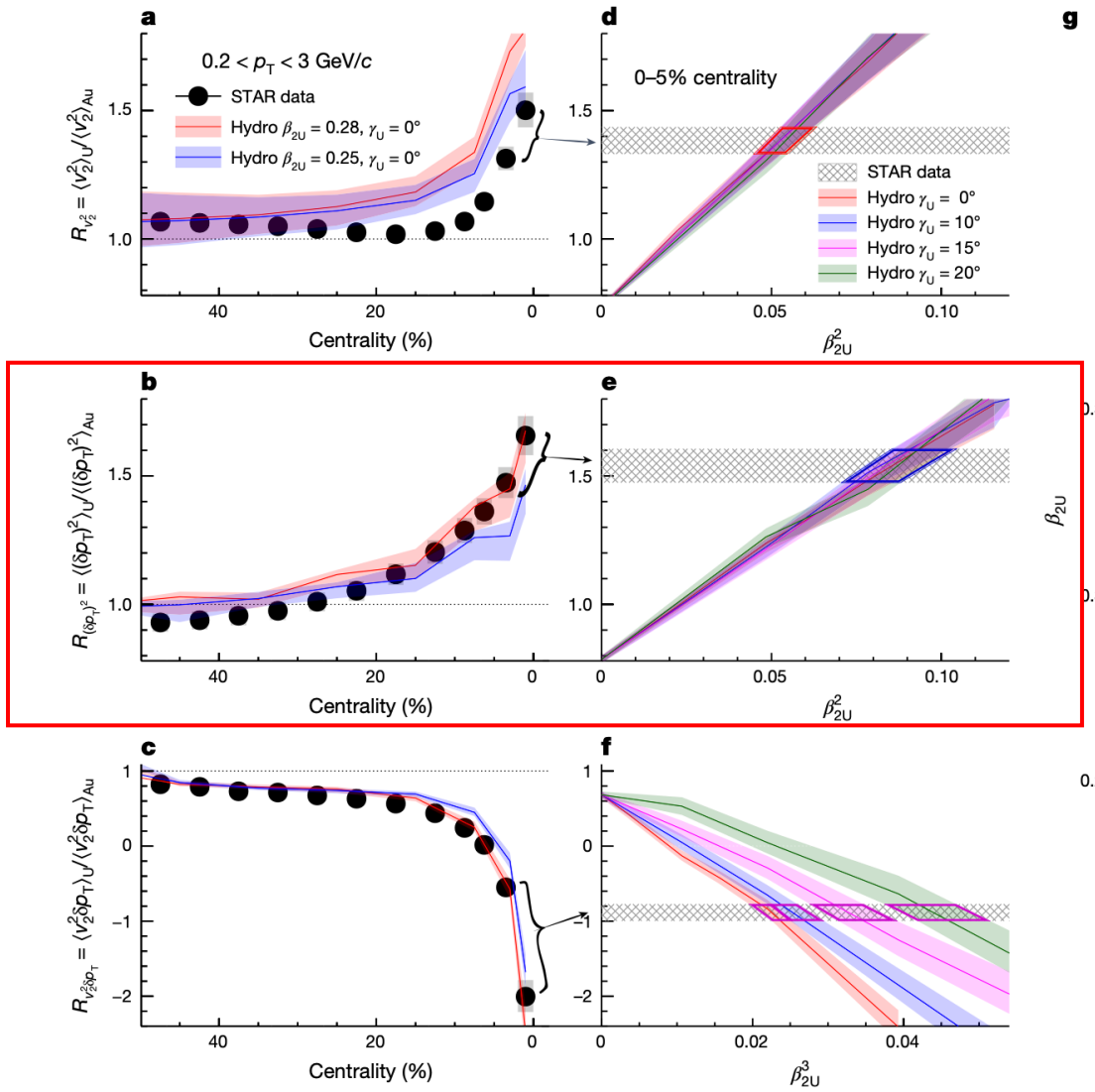


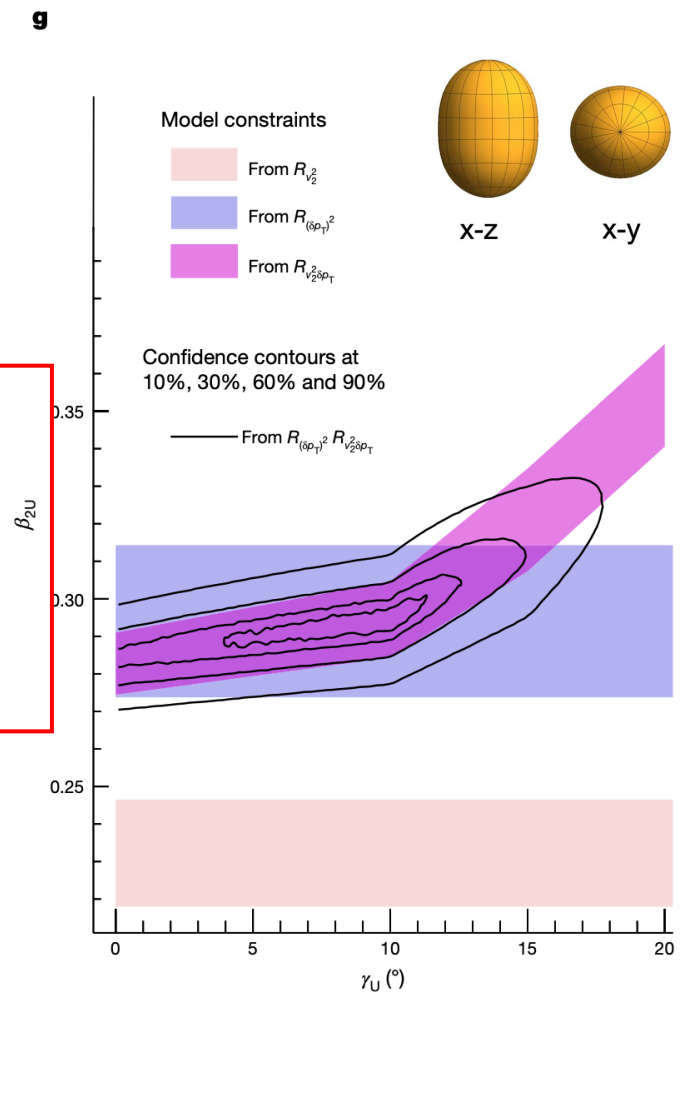
Tip-tip: $v_2 \searrow$ $p_T \nearrow$

Shape-frozen like a snapshot during nuclear crossing (10^{-25}s << rotational time scale 10^{-21}s)
probe entire mass distribution in the intrinsic frame via multi-point correlations

Constraining the ground-state ^{238}U: $\beta_{2,U}$ and γ_U

STAR, *Nature 635, 67-72 (2024)*





Sufficient precision is achieved from ratios in ultra-central collisions

Relation confirmed by hydro

$$R_{(v_2^2)} \approx 1 + \frac{b_1}{a_1}\beta_2^2,$$
$$R_{\langle(\delta p_T)^2\rangle} \approx 1 + \frac{b_2}{a_2}\beta_2^2,$$
$$R_{\langle v_2^2 \delta p_T\rangle} \approx 1 - \frac{b_3}{a_3}\beta_2^3\cos(3\gamma)$$

High-energy estimate
(*IP-Glasma+MUSIC* and *Trajectum*)

$$\beta_{2U} = 0.286 \pm 0.025$$
$$\gamma_U = 8.5^\circ \pm 4.8^\circ$$

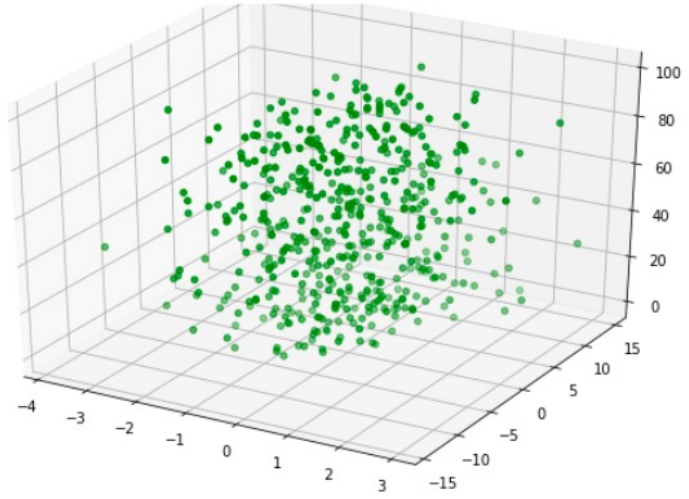
low-energy estimate:

$$\beta_{2U} = 0.287 \pm 0.007$$
$$\gamma_U = 6^\circ - 8^\circ$$

A large deformation with a slight deviation from axial symmetry in the nuclear ground-state

New observables: mean transverse momentum fluctuations

$f\left(p_{x1}, p_{y1}, p_{z1}, p_{x2}, p_{y2}, p_{z2} \ldots\right)$



Event-by-event temperature fluctuations

J. Jia, S. Huang, C. Zhang, *PRC 105 , 014906 (2022)*
S. Bhatta, C. Zhang, J. Jia, *PRC106, L031901 (2022)*
C. Zhang, A. Behera, S. Bhatta, J. Jia, *PLB 822, 136702 (2021)*

Mean: $\left\langle\left\langle p_{\mathrm{t}}\right\rangle\right\rangle=\frac{\sum_{k=1}^{N_{\text{events}}}\left\langle p_{\mathrm{t}}\right\rangle_k}{N_{\text{events}}}$ where $\left\langle p_{\mathrm{t}}\right\rangle_k=\frac{\sum_i w_i p_{\mathrm{t},i}}{\sum_i w_i}$

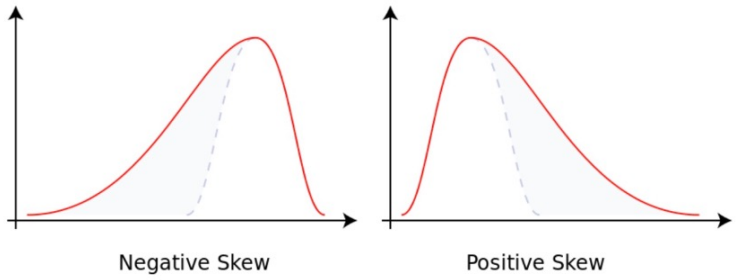
w_i is the detector efficiency

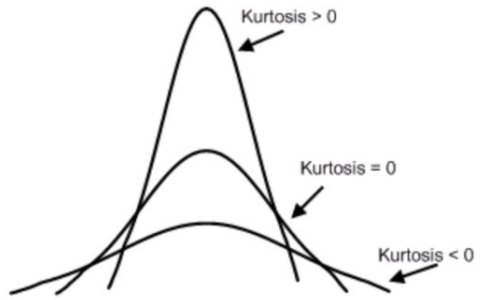
Variance: $\left\langle\left(\delta p_T\right)^2\right\rangle=\frac{\sum_i \sum_{j \neq i} \omega_i \omega_j\left(p_{T,i}-\left\langle\left[p_T\right]\right\rangle\right)\left(p_{T,j}-\left\langle\left[p_T\right]\right\rangle\right.}{\sum_i \sum_{j \neq i} \omega_i \omega_j}$,

Skewness: $\left\langle\left(\delta p_T\right)^3\right\rangle=\frac{\sum_{i, j \neq i, k \neq j \neq i} \omega_i \omega_j \omega_k\left(p_{T,i}-\left\langle\left[p_T\right]\right\rangle\right)\left(p_{T,j}-\left\langle\left[p_T\right]\right\rangle\right)\left(\left(p_{T,k}-\left\langle\left[p_T\right]\right\rangle\right)\right.}{\sum_{i, j \neq i, k \neq j \neq i} \omega_i \omega_j \omega_k}$,

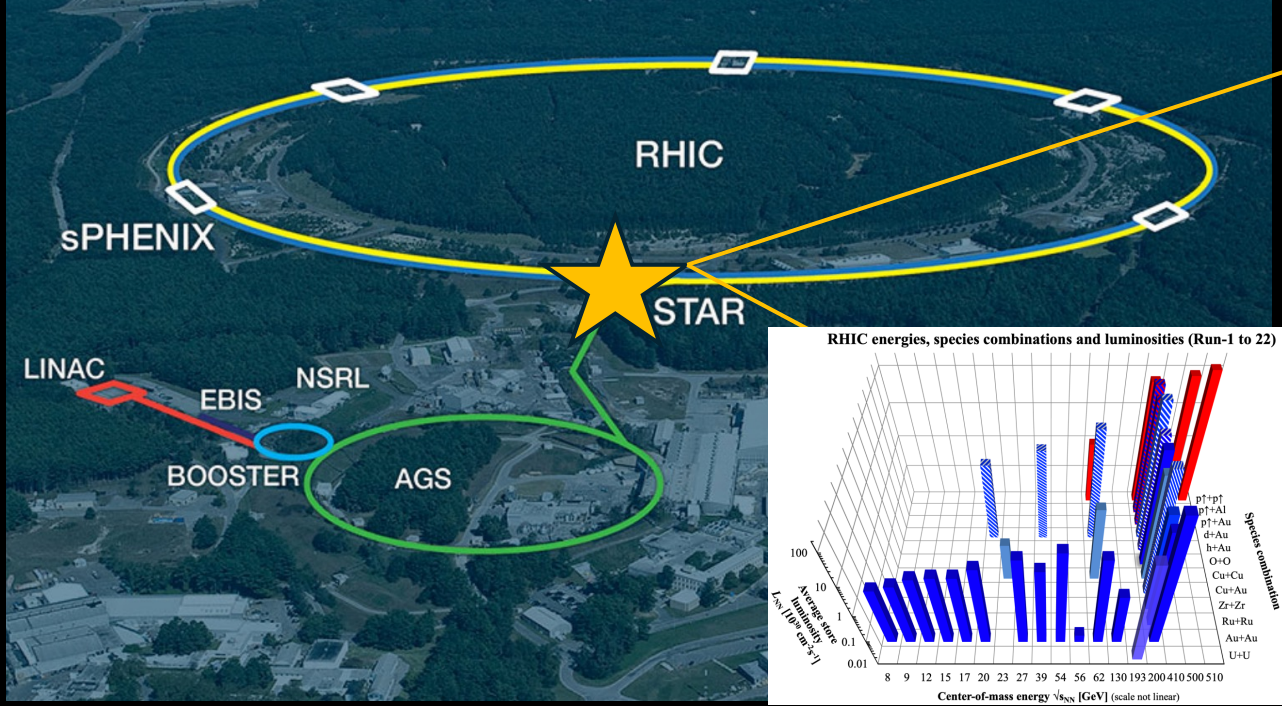
Kurtosis: $\left\langle\left(\delta p_T\right)^4\right\rangle=\frac{\sum_{i, j \neq i, k \neq j \neq i, l \neq k \neq j \neq i} \omega_i \omega_j \omega_k \omega_l\left(p_{T,i}-\left\langle\left[p_T\right]\right\rangle\right)\left(p_{T,j}-\left\langle\left[p_T\right]\right\rangle\right)\left(\left(p_{T,k}-\left\langle\left[p_T\right]\right\rangle\right)\right)\left(p_{T,l}-\left\langle\left[p_T\right]\right\rangle\right)}{\sum_{i, j \neq i, k \neq j \neq i, l \neq k \neq j \neq i} \omega_i \omega_j \omega_k \omega_l}$

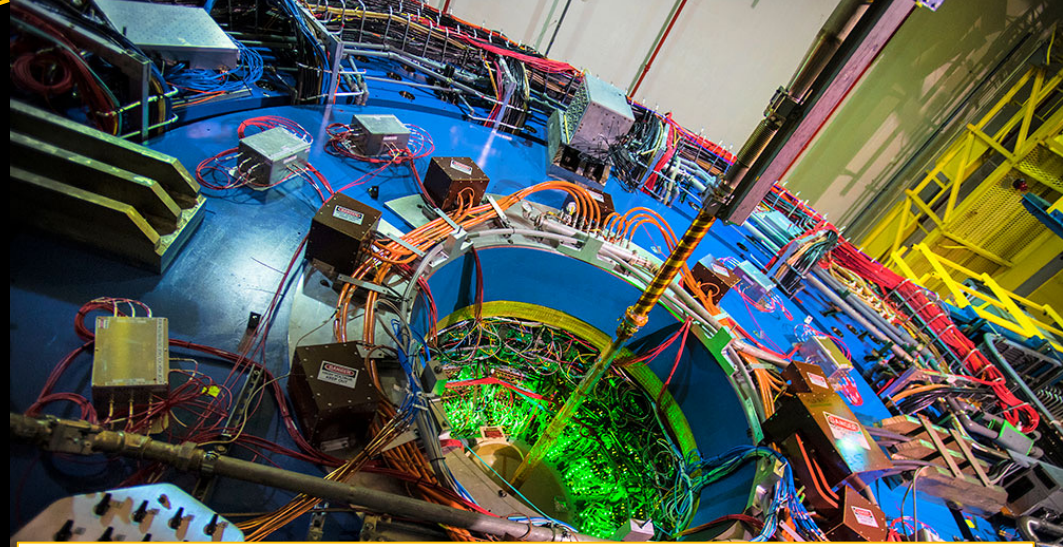
Related to the entropy of the initial source presumably deposited early in the collision before thermalization and interactions with QGP



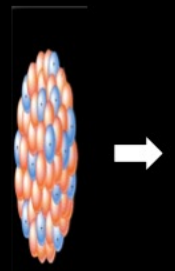


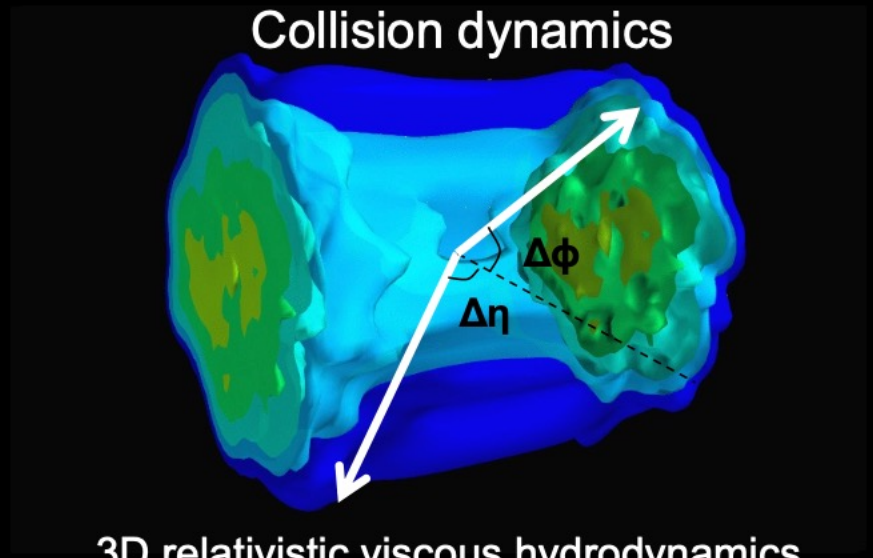
S. Gavin, *PRL 92, 162301 (2004)*

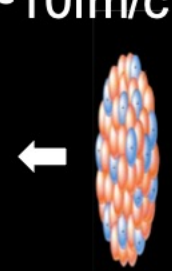




1) large, uniform acceptance at mid-rapidity
2) A vast number of emitted final state hardons
3) capability to access nuclear structures in different collisions…







t~10fm/c =10^{-22} s

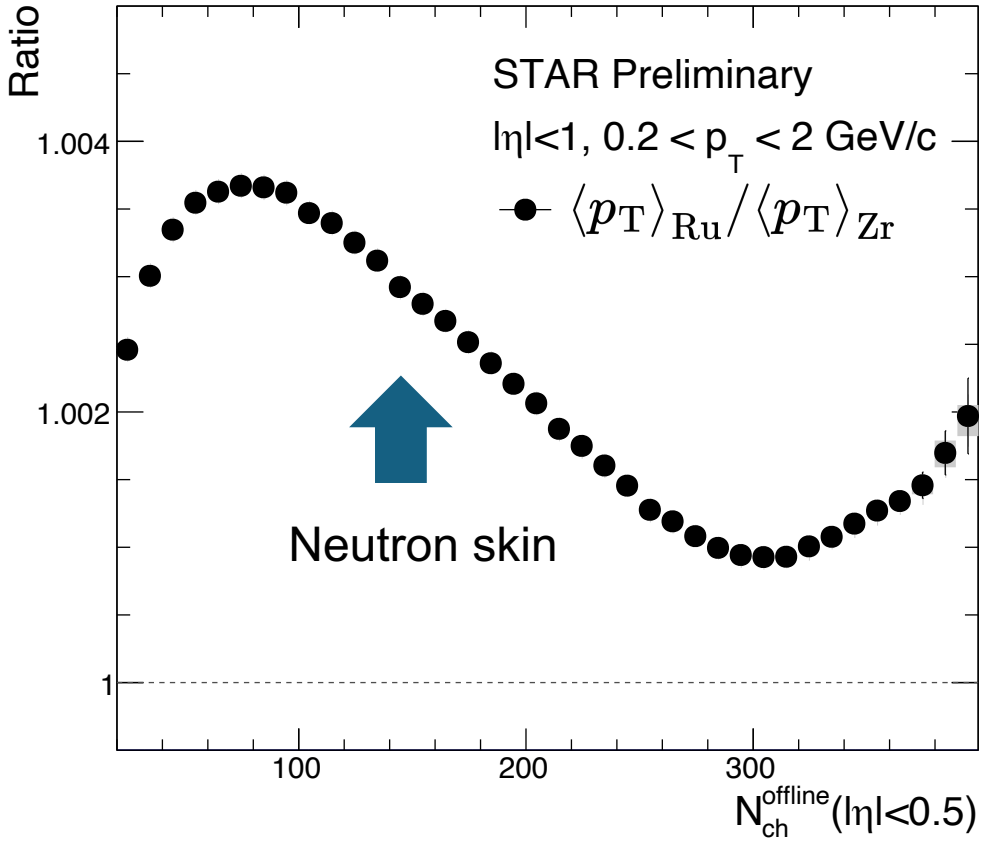
Credit: Bjoern Schenke

❑ Imaging nuclear structure in high-energy collisions

I. Nuclear structure in ^{238}U, ^{96}Ru/^{96}Zr

$\langle p_T \rangle$ sensitive to nuclear skin

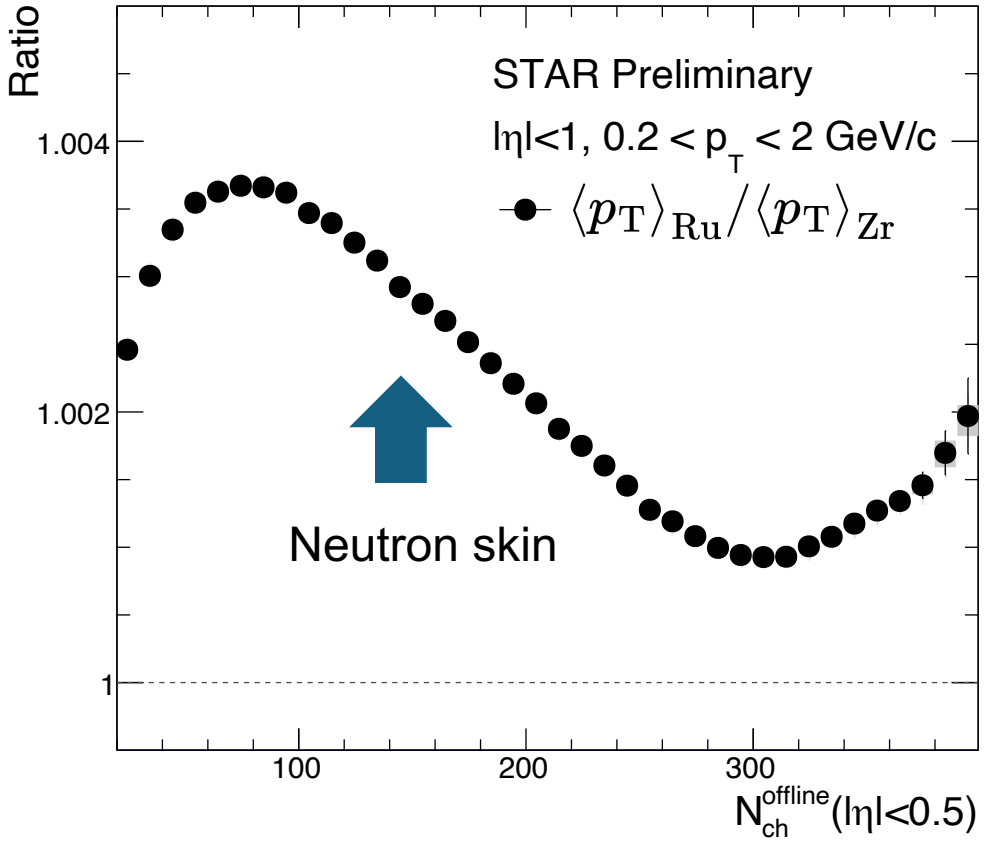
C. Zhang (STAR), *QM2022*



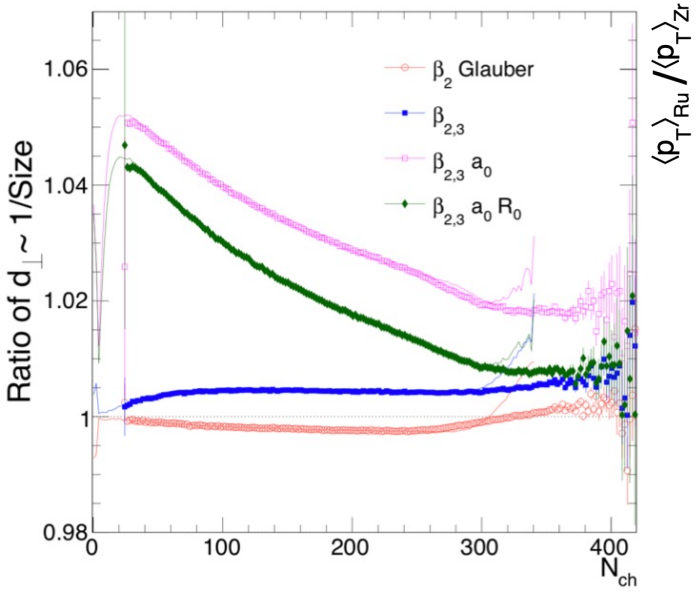
The nonmonotonic trend reflects the neutron skin effect.

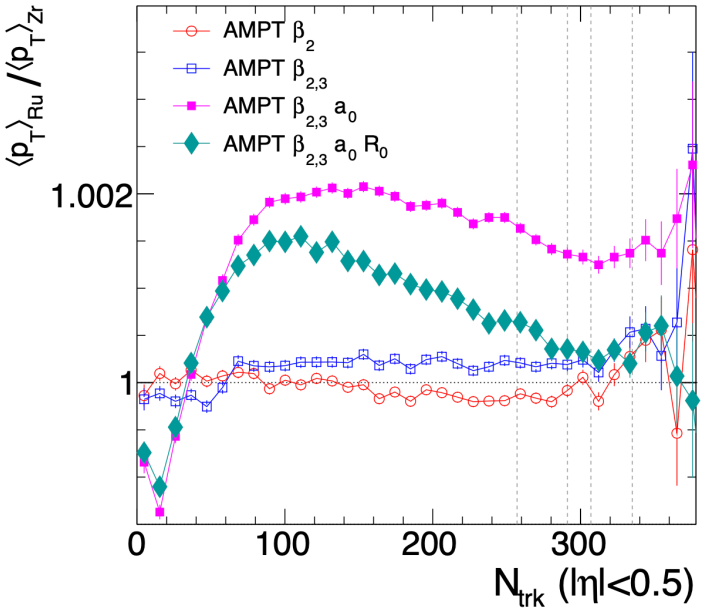
$\langle p_T \rangle$ sensitive to nuclear skin

C. Zhang (STAR), *QM2022*



Initial-state Glauber and final-state AMPT



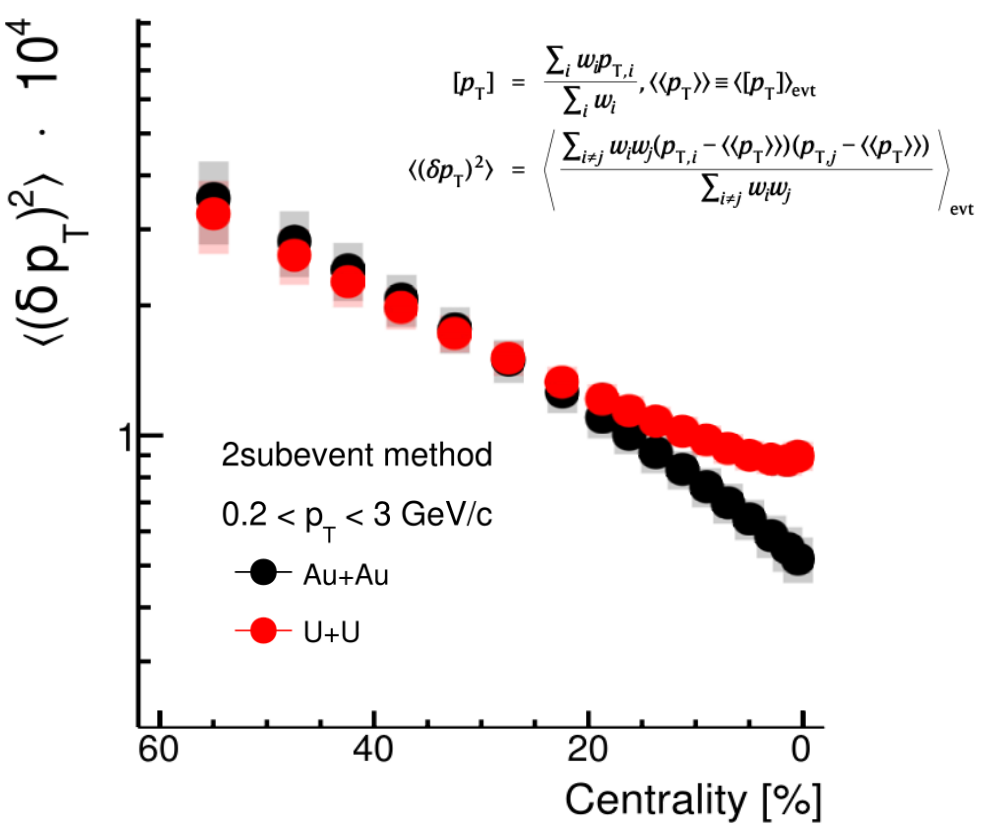


J. Jia, *PRC 105, 044905 (2022)*

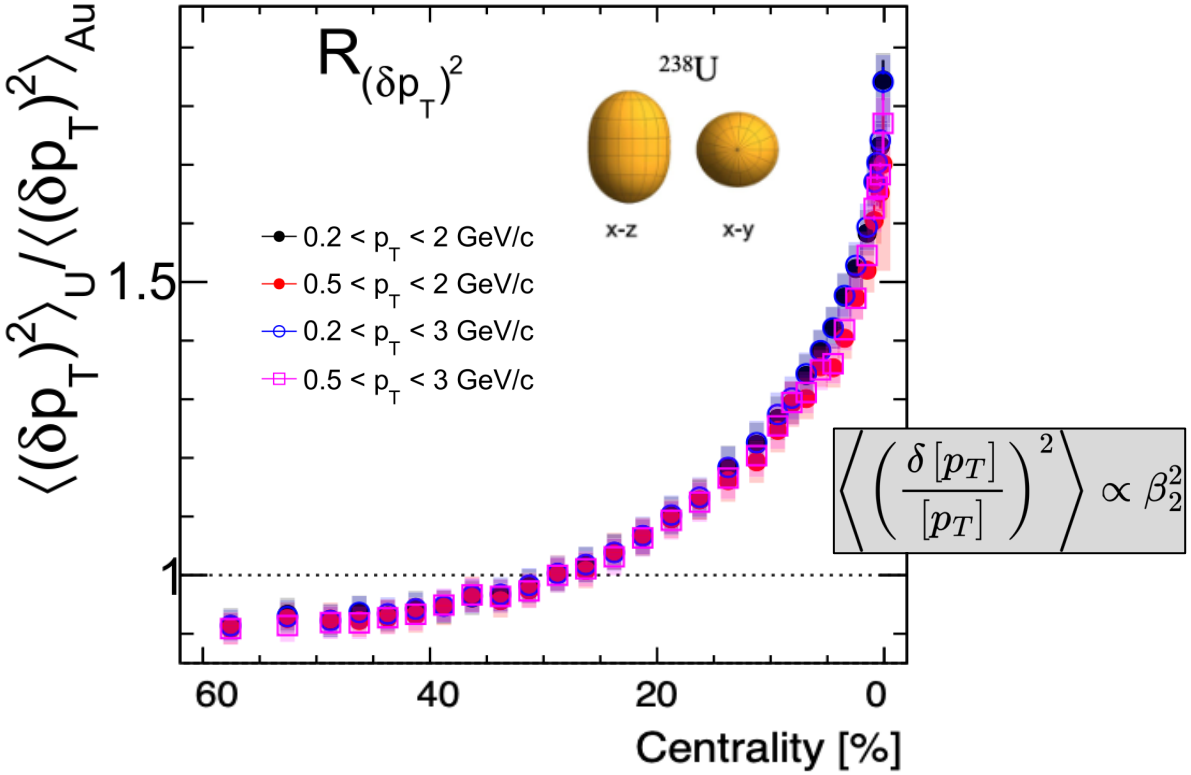
The nonmonotonic trend reflects the neutron skin effect.

$\langle(\delta p_T)^2\rangle$ sensitive to nuclear deformation

STAR, *Nature 67, 635 (2025)*



STAR, *Rep. Prog. Phys. 88,108601 (2025)*



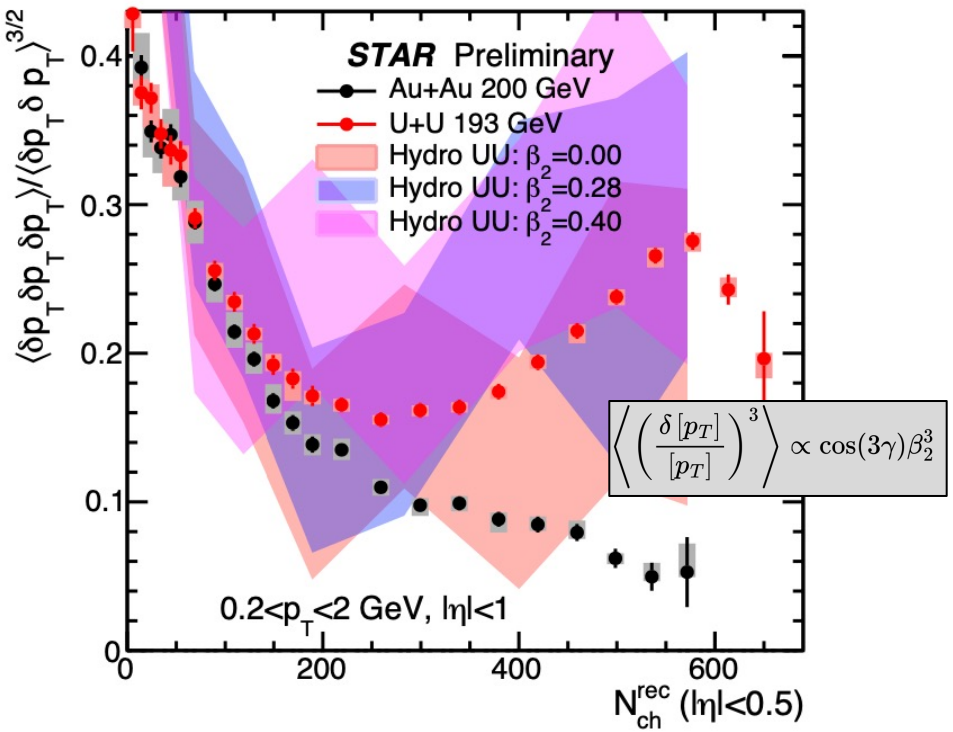
large enhancement in mean and variance ⟶ size fluctuations enhanced

A good probe to image nuclear deformation.

ALICE, *PLB 850, 138541 (2024);* ATLAS, *PRL 133, 252301 (2024);* G. Giacalone, J. Jia, C. Zhang, *PRL 127, 242301 (2021)*

$\langle(\delta p_T)^3\rangle$ and $\langle(\delta p_T)^4\rangle$ sensitive to nuclear deformation

C. Zhang (STAR), *IJMPE 32, 2341001 (2023)*



Independence source model: following $1/N_s^{n-1}$ within power-law decrease in high-order

M. Cody et. al., *Phys. Rev. C 107, (2023)*

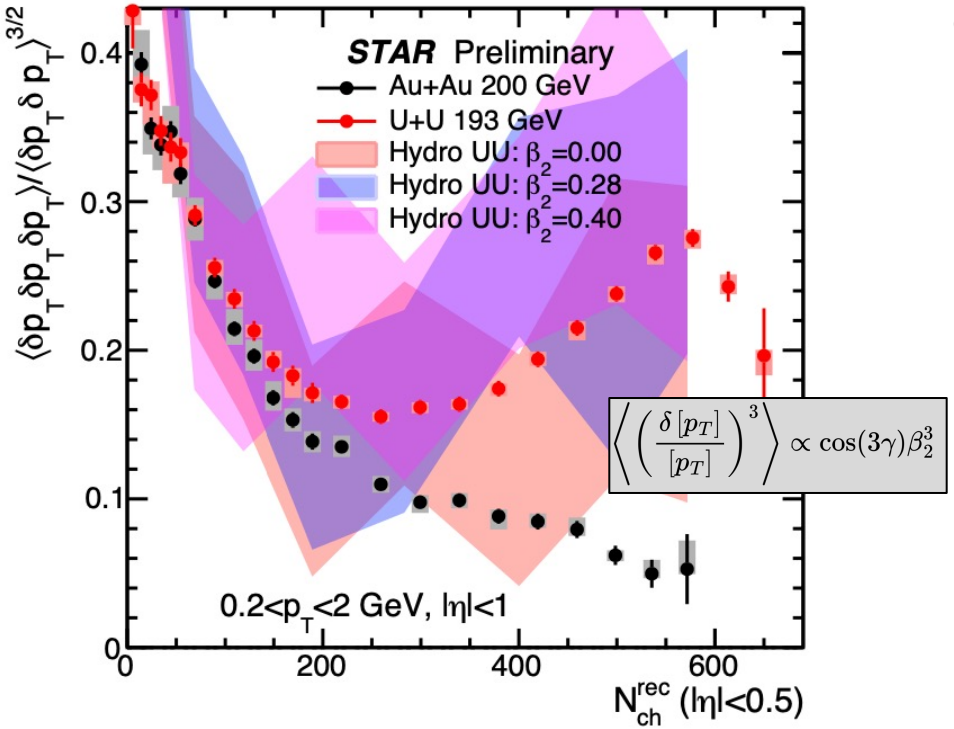
Size fluctuations enhanced: large enhancement in skewness and **sign-change** in kurtosis

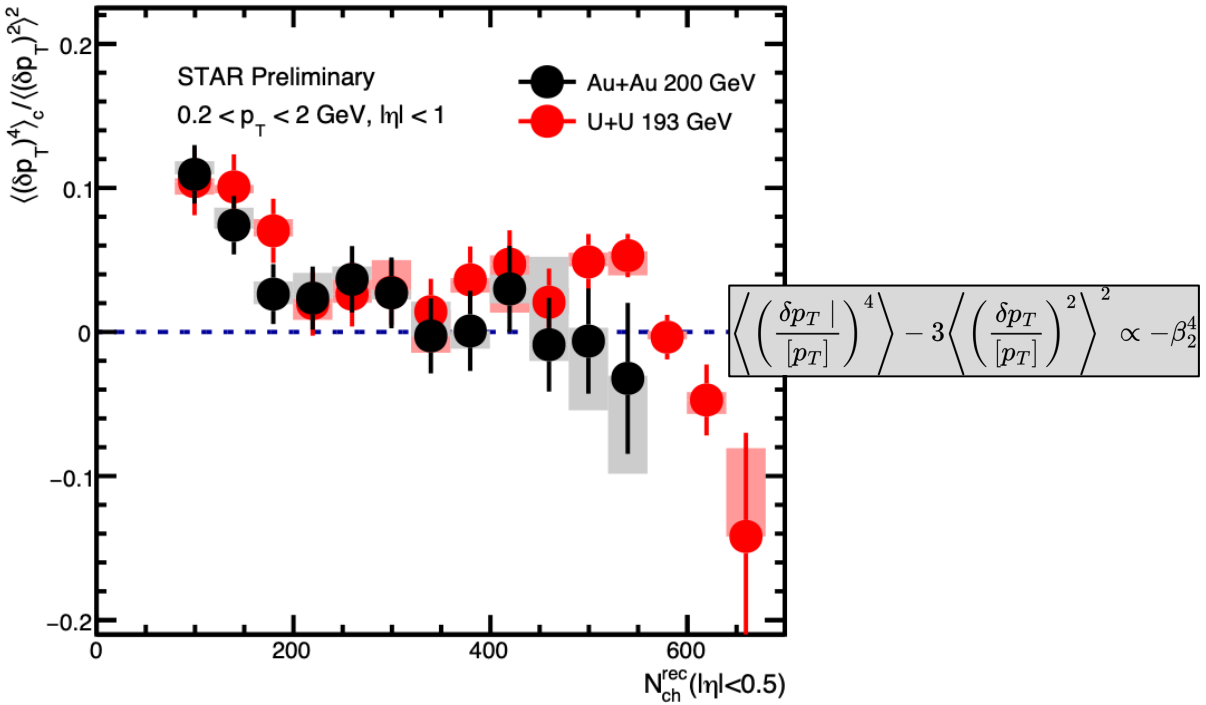
Confirmed by hydro, will update the hydro statistics.

ALICE, *PLB 850, 138541 (2024);* ATLAS, *PRL 133, 252301 (2024);* G. Giacalone, J. Jia, C. Zhang, *PRL 127, 242301 (2021)*

$\langle(\delta p_T)^3\rangle$ and $\langle(\delta p_T)^4\rangle$ sensitive to nuclear deformation

C. Zhang (STAR), *IJMPE 32, 2341001 (2023)*





Independence source model: following $1/N_s^{n-1}$ within power-law decrease in high-order

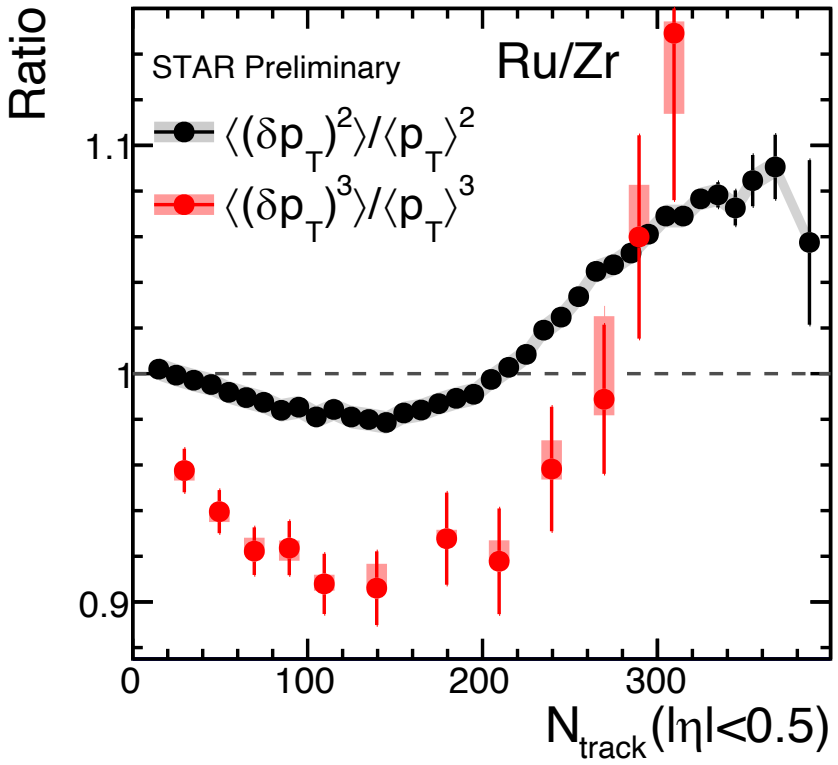
M. Cody et. al., *Phys. Rev. C 107, (2023)*

Size fluctuations enhanced: large enhancement in skewness and **sign-change** in kurtosis

Confirmed by hydro, will update the hydro statistics.

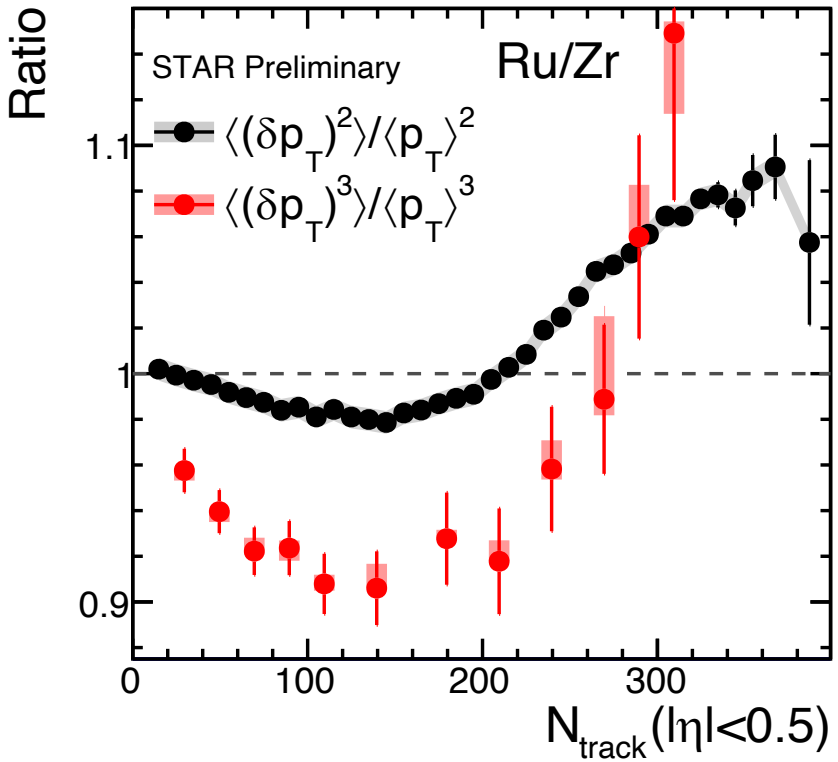
ALICE, *PLB 850, 138541 (2024);* ATLAS, *PRL 133, 252301 (2024);* G. Giacalone, J. Jia, C. Zhang, *PRL 127, 242301 (2021)*

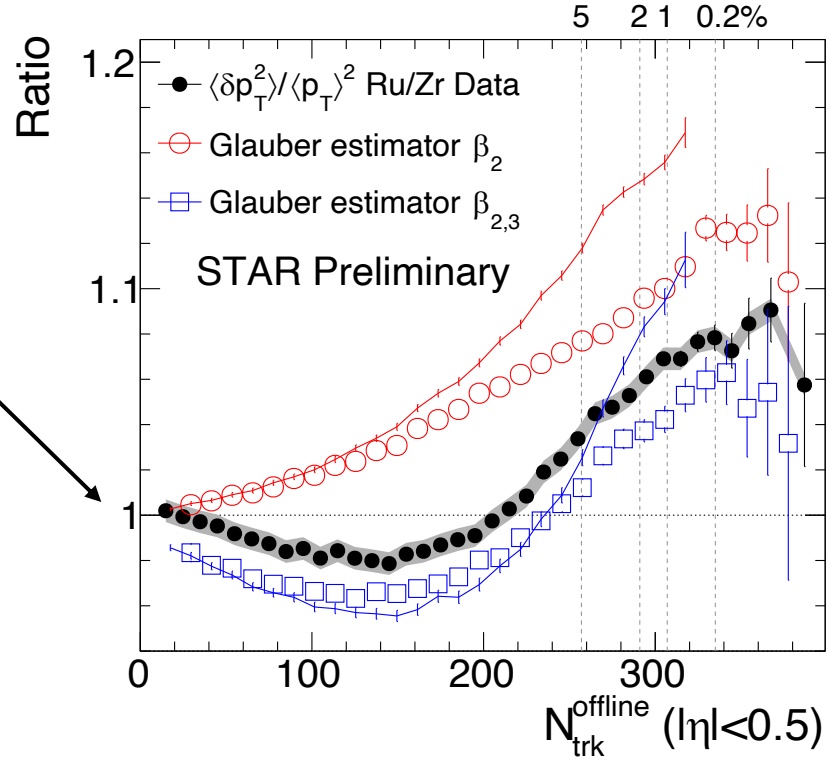
$\langle(\delta p_T)^2\rangle$ and $\langle(\delta p_T)^3\rangle$ are sensitive to nuclear deformation in ^{96}Ru and ^{96}Zr



Octupole deformation: large enhancement in skewness and sign-change in kurtosis

$\langle(\delta p_T)^2\rangle$ and $\langle(\delta p_T)^3\rangle$ are sensitive to nuclear deformation in ^{96}Ru and ^{96}Zr





$$\left\langle \left(\frac{\delta [p_T]}{[p_T]} \right)^2 \right\rangle \propto \beta_2^2$$

$$\left\langle \left(\frac{\delta [p_T]}{[p_T]} \right)^3 \right\rangle \propto \cos(3\gamma)\beta_2^3$$

$$\frac{\langle \delta p_T^2 \rangle_{\mathrm{Ru}}}{\langle \delta p_T^2 \rangle_{\mathrm{Zr}}} \approx 1 + \frac{b_0}{a_0}\left(\beta_{2,\mathrm{Ru}}^2 - \beta_{2,\mathrm{Zr}}^2\right) - \frac{b_{0,3}}{a_0}\beta_{3,\mathrm{Zr}}^2$$

Cancelation expected in non-central collisions

C. Zhang, J. Jia, *PRL 128, 022301 (2022)*

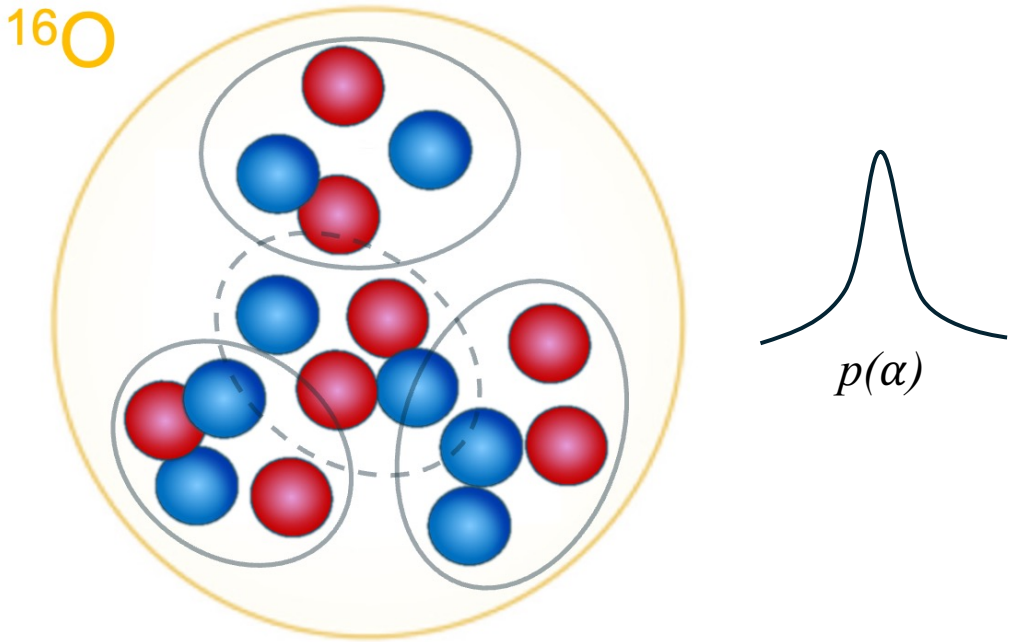
Octupole deformation: large enhancement in skewness and sign-change in kurtosis

II. Geometry effect and subnucleon fluctuations in ^{16}O

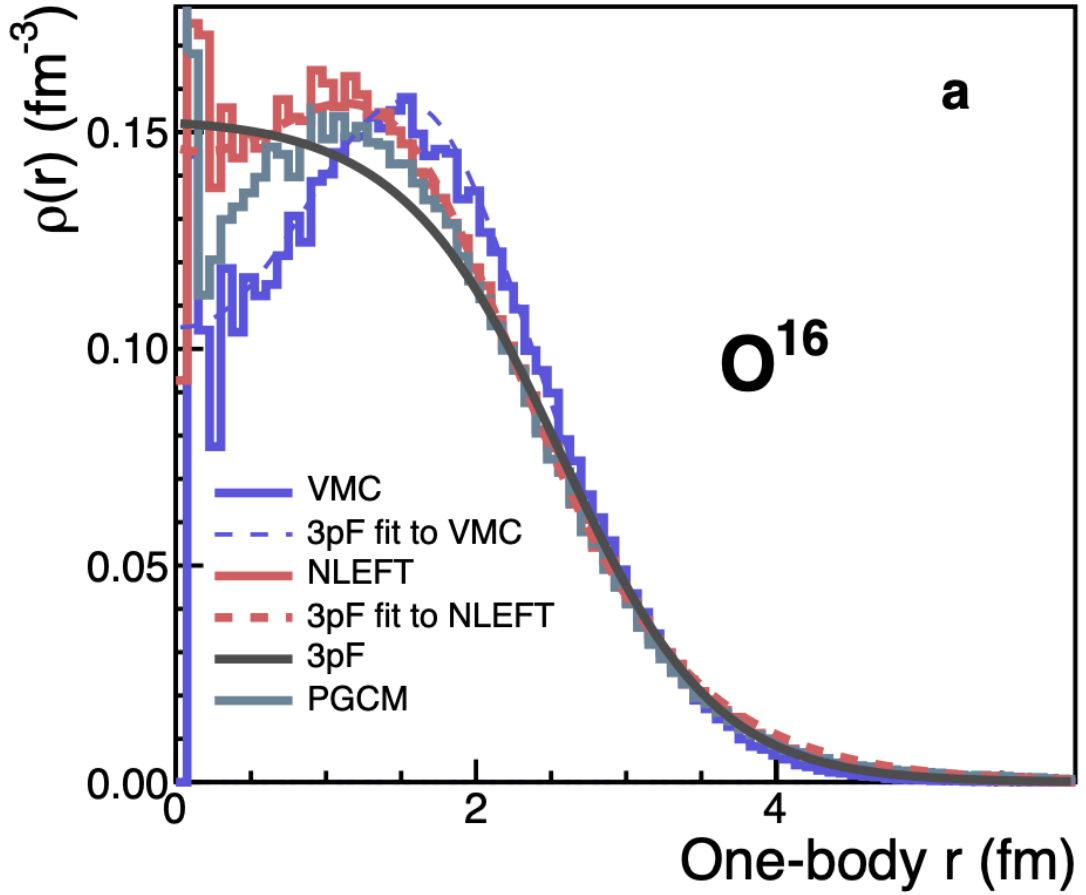
Light nuclei: geometry and many-nucleon correlations

"Double magic number" in $^{16}_{8}O$ nuclei, possible alpha cluster in low-energy studies.

NN correlation (cluster pattern)



ab initio calculations

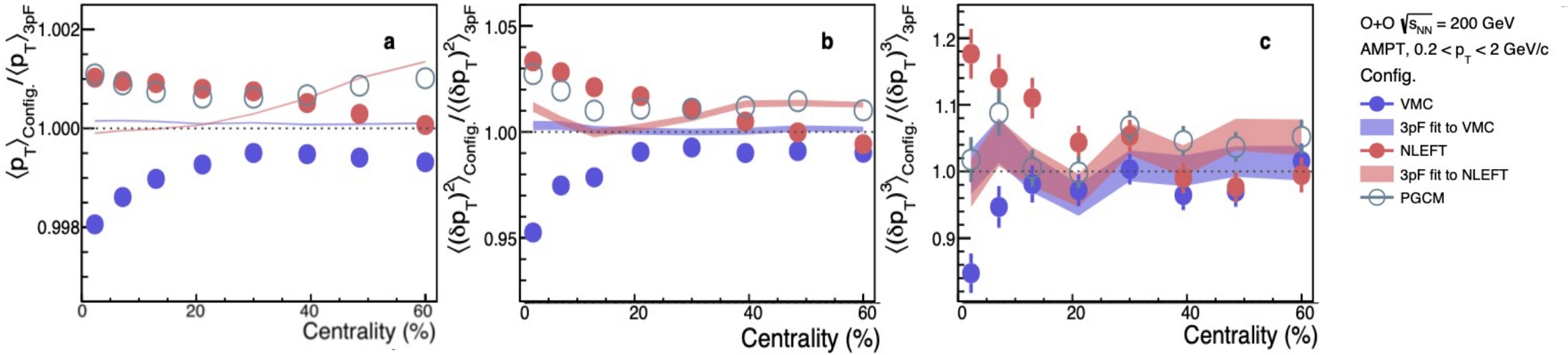


Nuclear inputs: VMC / AFDMC, NLEFT, and PGCM. C. Zhang, J. Chen, G. Giacalone, S. Huang, J. Jia, Y.-G. Ma, *PLB 862, 139322 (2025)*

Ab-initio NN correlations and their impact on p_T fluctuations

C. Zhang, J. Chen, G. Giacalone, S. Huang, J. Jia, Y.-G. Ma, *PLB 862, 139322 (2025)*

Multiple final-state observables

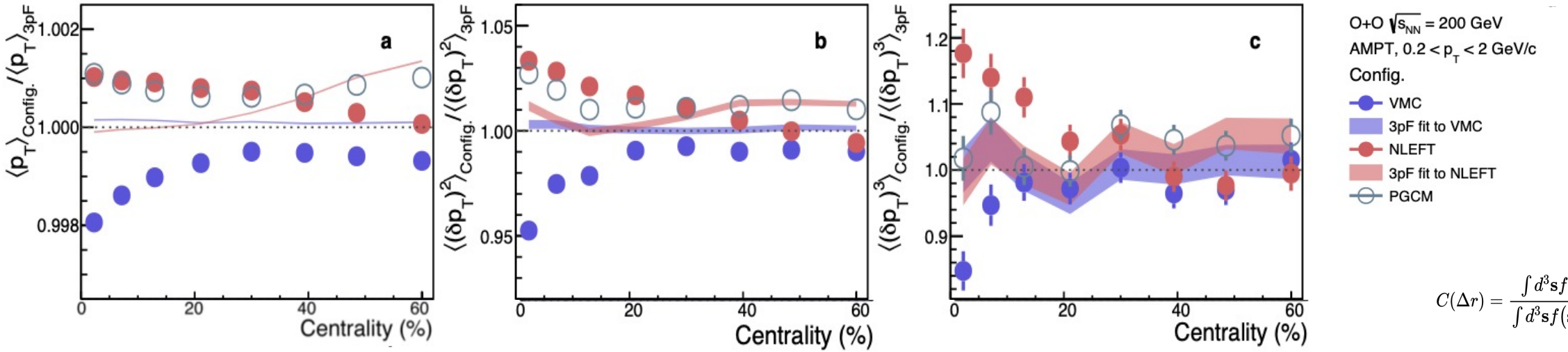


- 3pF as the baseline can NOT capture the NN correlations.
- Distinct differences are observed between VMC and NLEFT/PGCM.
- Central collision is prominent.

Ab-initio NN correlations and their impact on p_T fluctuations

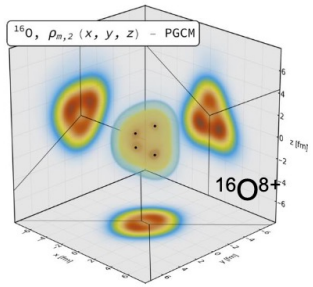
C. Zhang, J. Chen, G. Giacalone, S. Huang, J. Jia, Y.-G. Ma, *PLB 862, 139322 (2025)*

Multiple final-state observables

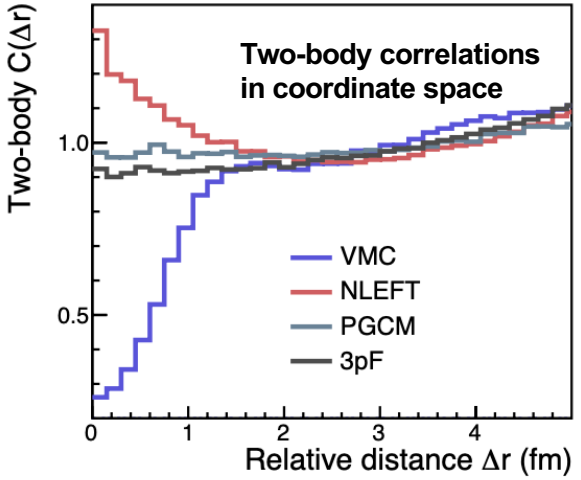


$$C(\Delta r) = \frac{\int d^3\mathbf{s} f\left(\mathbf{s}+\frac{\mathbf{r}}{2},\mathbf{s}-\frac{\mathbf{r}}{2}\right)}{\int d^3\mathbf{s} f\left(\mathbf{s}+\frac{\mathbf{r}}{2}\right) f\left(\mathbf{s}-\frac{\mathbf{r}}{2}\right)}$$

- 3pF as the baseline can NOT capture the NN correlations.
- Distinct differences are observed between VMC and NLEFT/PGCM.
- Central collision is prominent.



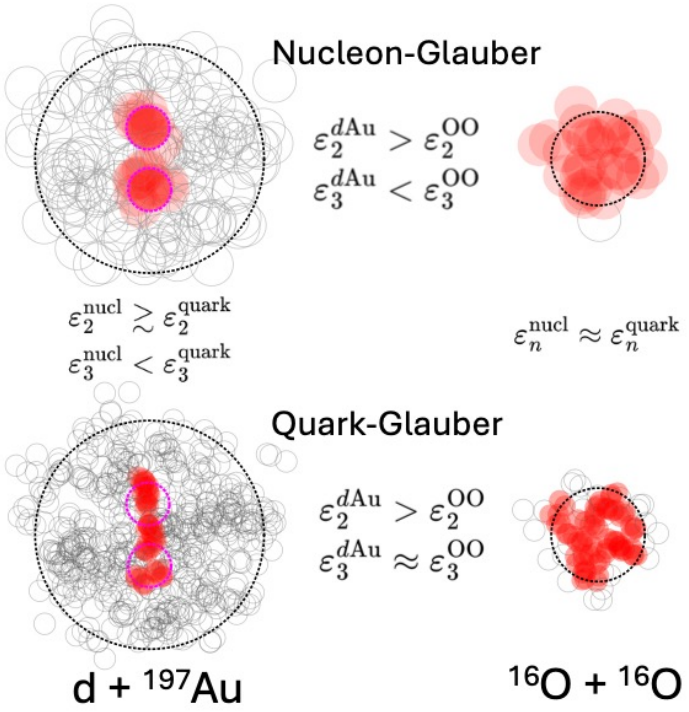
α cluster



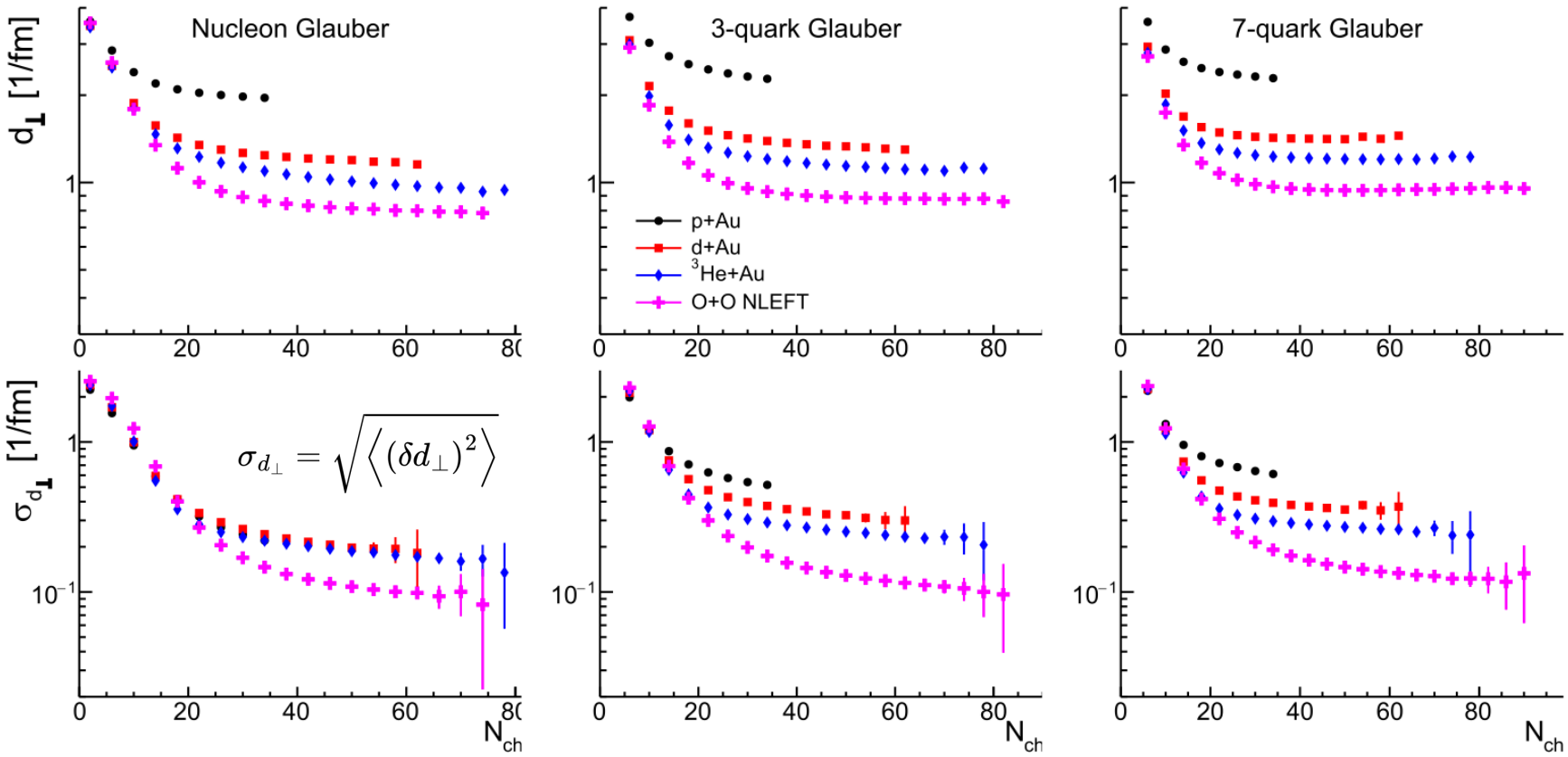
Nucleon/sub-nucleon fluctuation vs. *NN* correlations

$d_\perp = 1/\sqrt{[x^2]\,[y^2]}$ $\quad \delta d_\perp = d_\perp - \langle d_\perp \rangle$

S. Huang, J. Jia, C. Zhang, *PLB 870, 139926 (2025)*



STAR, *2510.19645*



The variance of $[p_T]$ should be significantly enhanced in d+Au collisions compared to O+O collisions at the same N_{ch}.

$\sigma_{d\perp}$ values are similar among asymmetric collisions in the nucleon Glauber model, while they show a clear hierarchy in the quark-Glaubermodel.

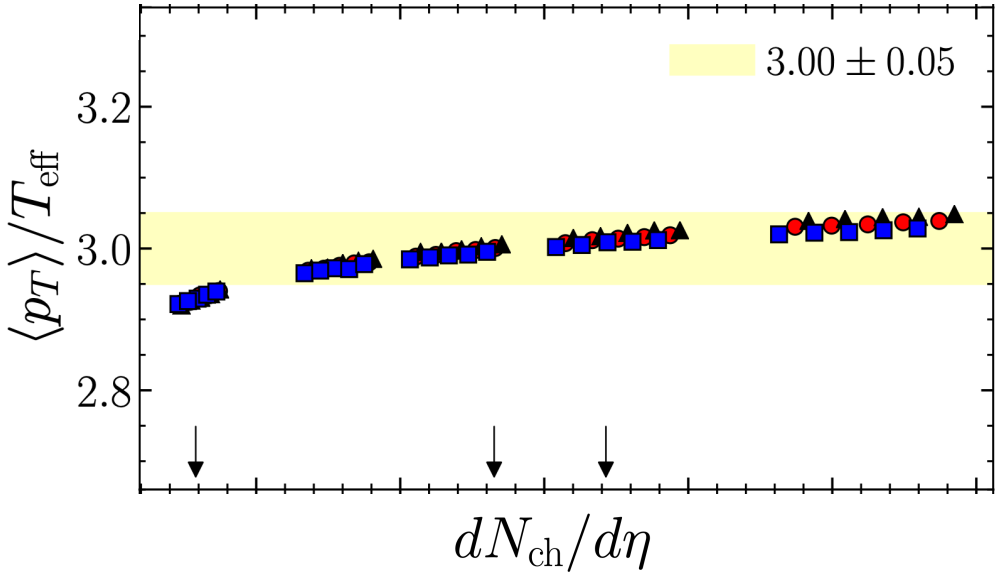
An independent test of geometry-driven interpretation of the radial flow.

❑ Probing QCD matter properties

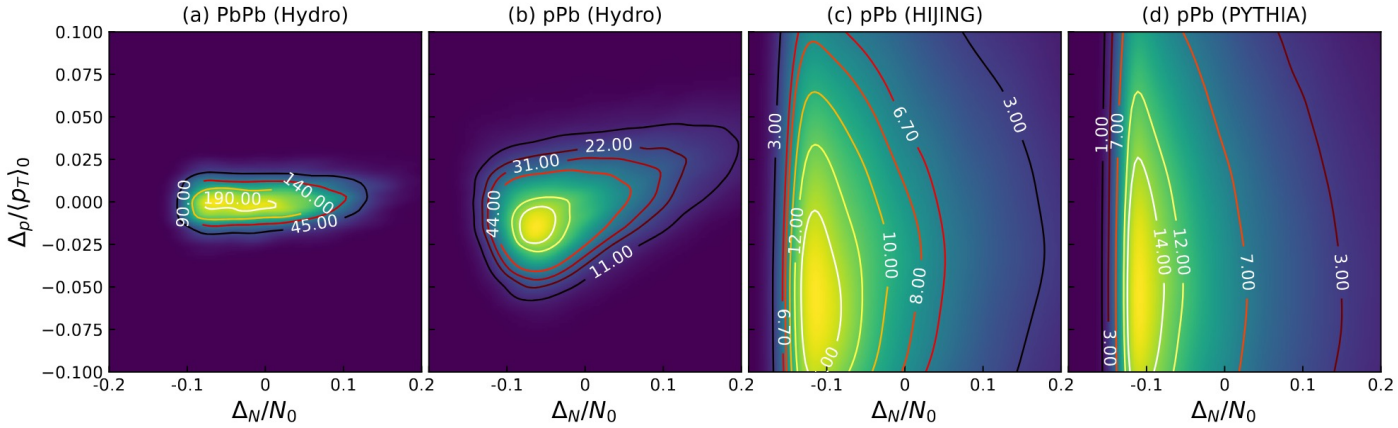
I. Second-order p_T fluctuation in ^{197}Au + ^{197}Au collisions at FXT energies

Momentum fluctuations and medium response

F. G. Gardim, A.V. Giannini, J. Y. Ollitrault., PLB 856, 138937 (2024)



Y.-S. Mu, L. Yan, X.-G. Huang, PRL 135, 162301 (2025)



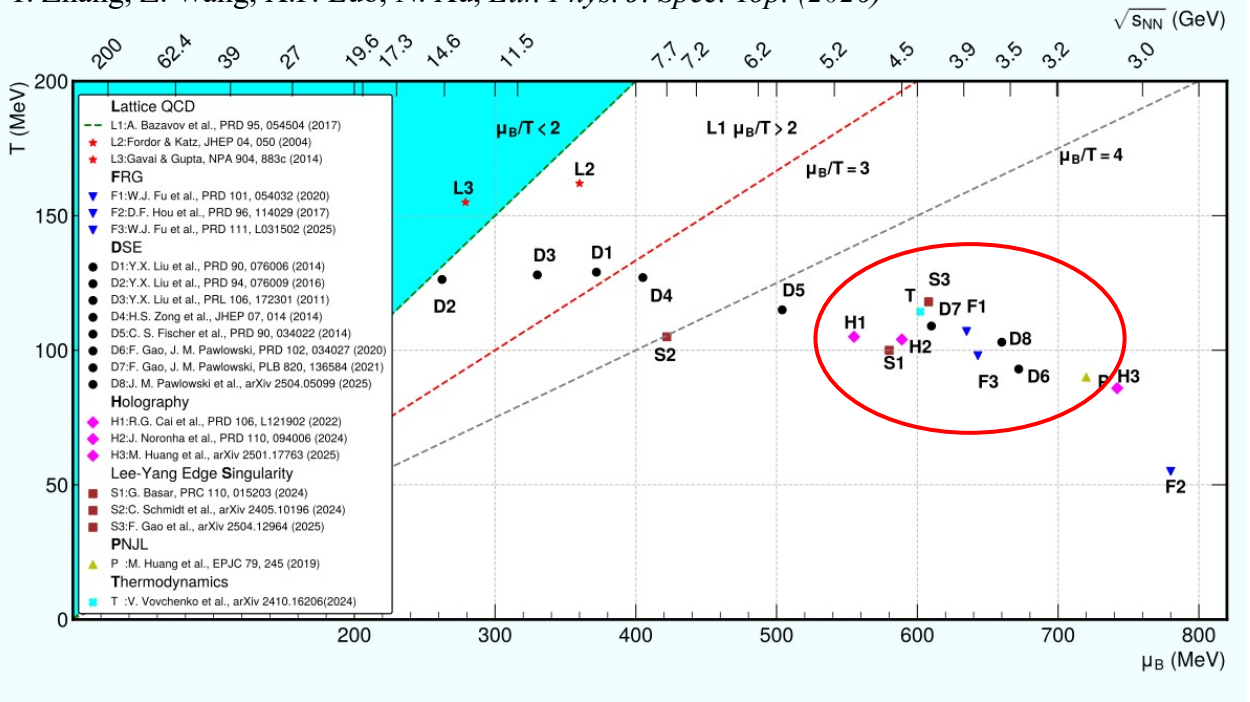
$$\frac{\Delta_p}{\langle p_T \rangle_0} = c_s^2 \frac{\Delta_N + \delta}{N_0} \qquad (c_s^2)^3 \frac{\{\Delta_N^3\}}{N_0^3} - 3(c_s^2)^2 \frac{\{\Delta_N^2 \Delta_p\}}{N_0^2 \langle p_T \rangle_0} + 3c_s^2 \frac{\{\Delta_N \Delta_p^2\}}{N_0 \langle p_T \rangle_0^2} - \frac{\{\Delta_p^3\}}{\langle p_T \rangle_0^3} = 0$$

- In ultra-central Pb–Pb collisions, $\langle p_T \rangle$ provides an approximate measure of the effective temperature
- Event-by-event fluctuations in $\langle p_T \rangle$, combined with multiplicity fluctuations, can provide information about the thermodynamic response of the QCD medium

May help constrain the QCD equation of state at high baryon density

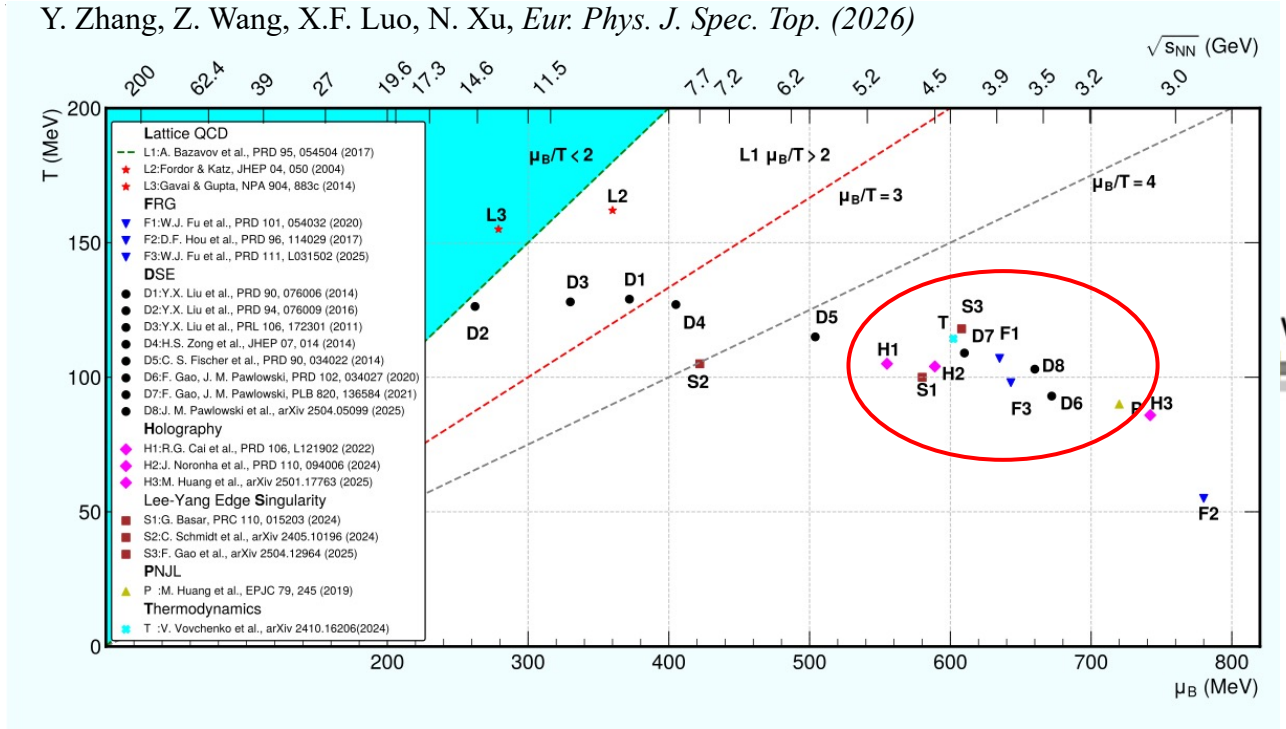
The BES-II Upgrades and fixed-target (FXT) mode

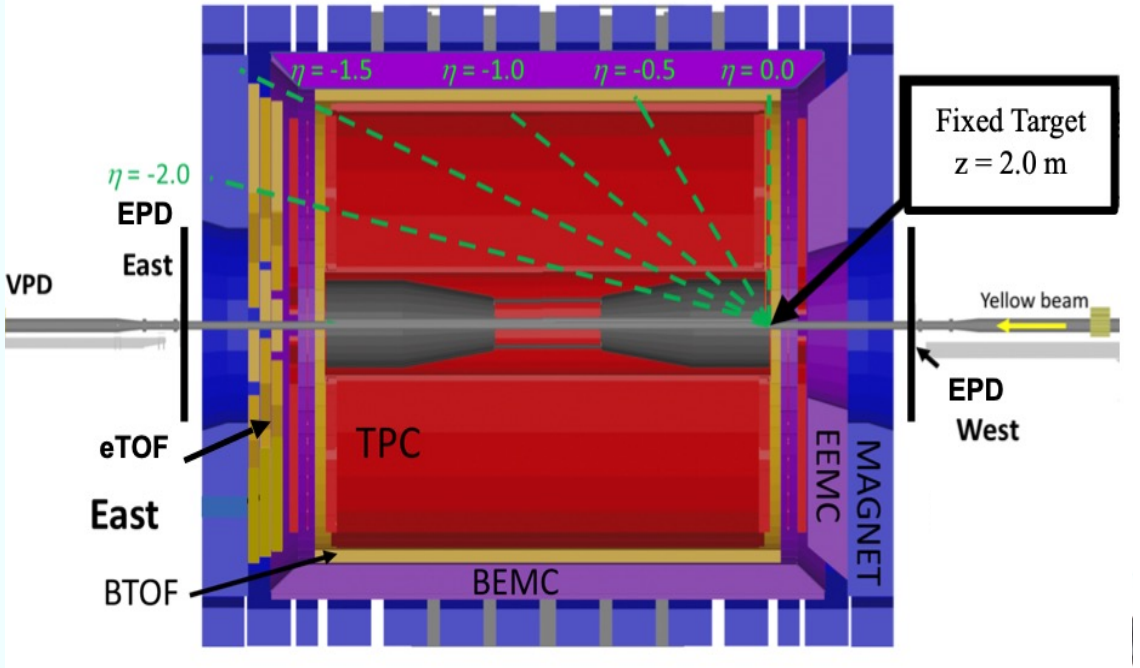
Y. Zhang, Z. Wang, X.F. Luo, N. Xu, *Eur. Phys. J. Spec. Top. (2026)*



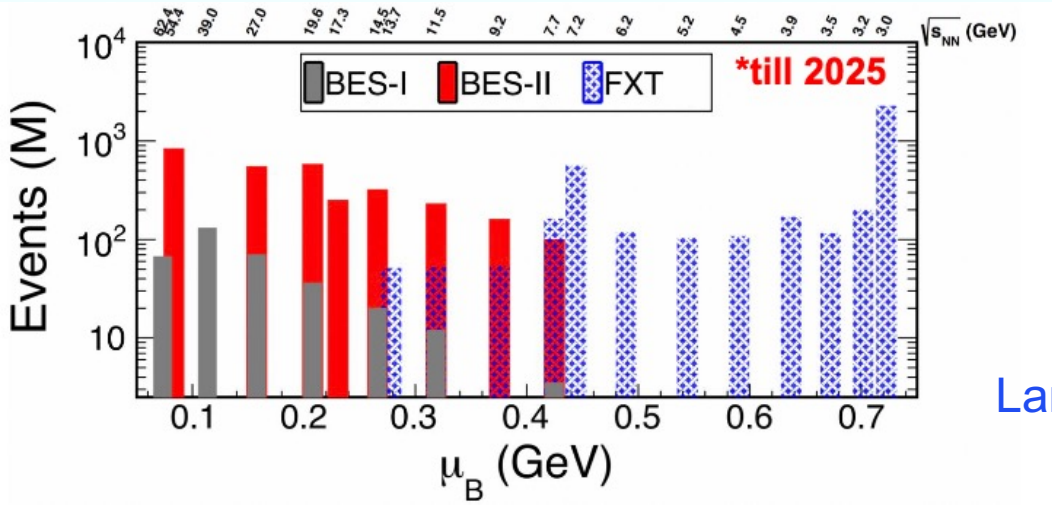
The BES-II Upgrades and fixed-target (FXT) mode

Y. Zhang, Z. Wang, X.F. Luo, N. Xu, *Eur. Phys. J. Spec. Top. (2026)*





Mid-rapidity for 3.0 GeV is y = 1.049

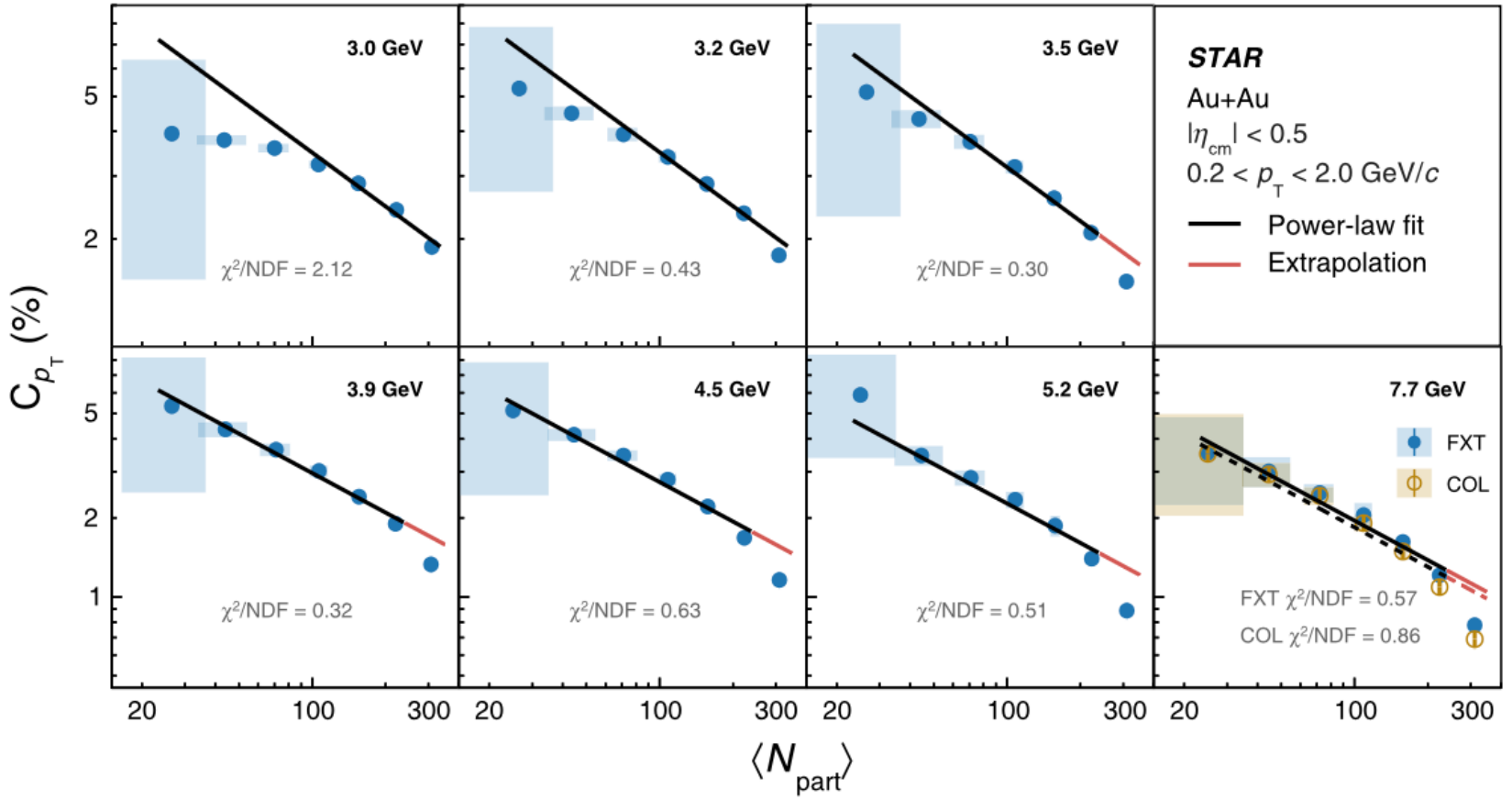


A strong convergence of predicted points within the 3–6 GeV energies

Large datasets with iTPC upgrade ~10 X BES-I

$\sqrt{\langle(\delta p_T)^2\rangle}/\langle\langle p_T\rangle\rangle$ vs centrality in FXT mode

STAR, *PRL 137, 132301 (2026)*

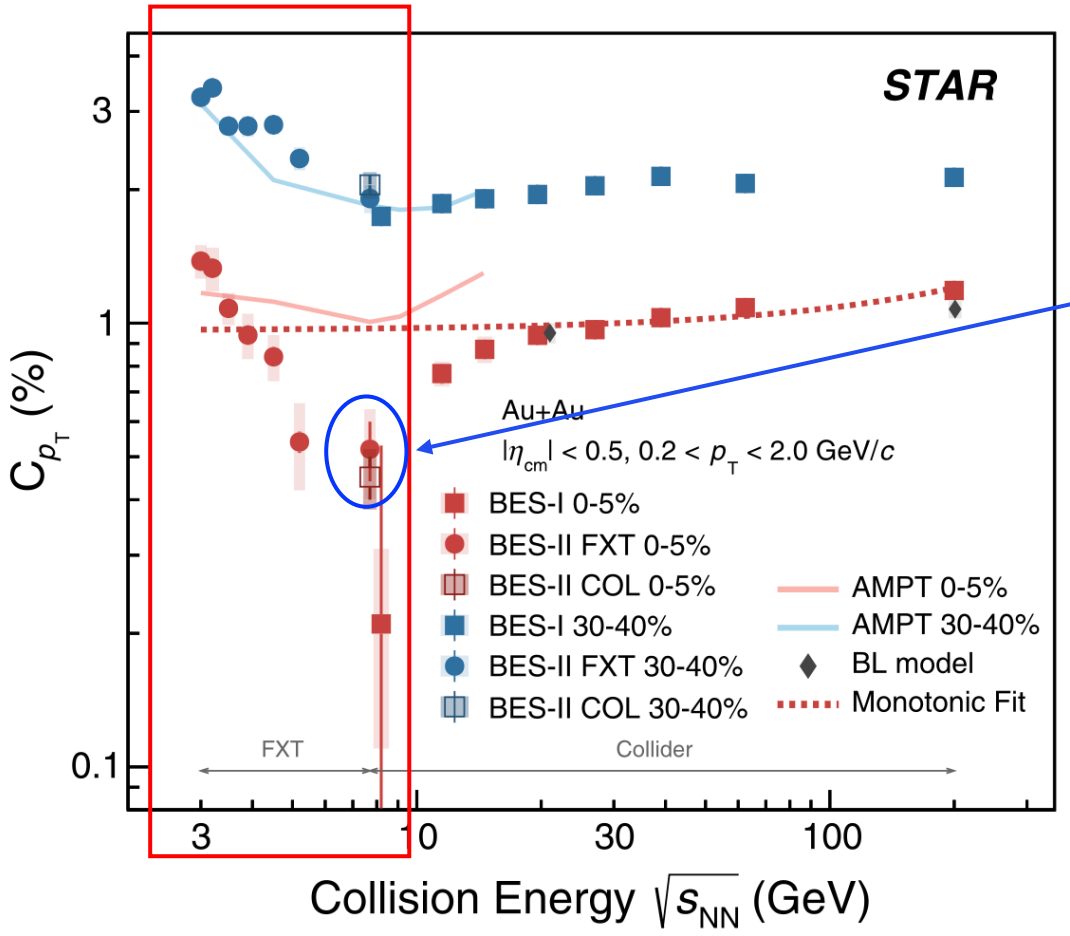


- Correlations larger in the peripheral collisions and decrease with centrality
- Measurements deviate from power-law behavior, implying that the centrality dependence does not follow a simple superposition scenario
- Independent of the collision mode: good agreement between measurements made at 7.7 GeV in FXT and collider modes.

Nonmonotonicity of $\sqrt{\langle(\delta p_T)^2\rangle}/\langle\langle p_T\rangle\rangle$ vs collision energy in FXT mode

μ_B ~ 400 - 600 MeV

STAR, *PRL 137, 132301 (2026)*



No acceptance effect: at 7.7 GeV, BES-II is consistent with BES-I.

Useful for constraining EoS and understanding the phase diagram.

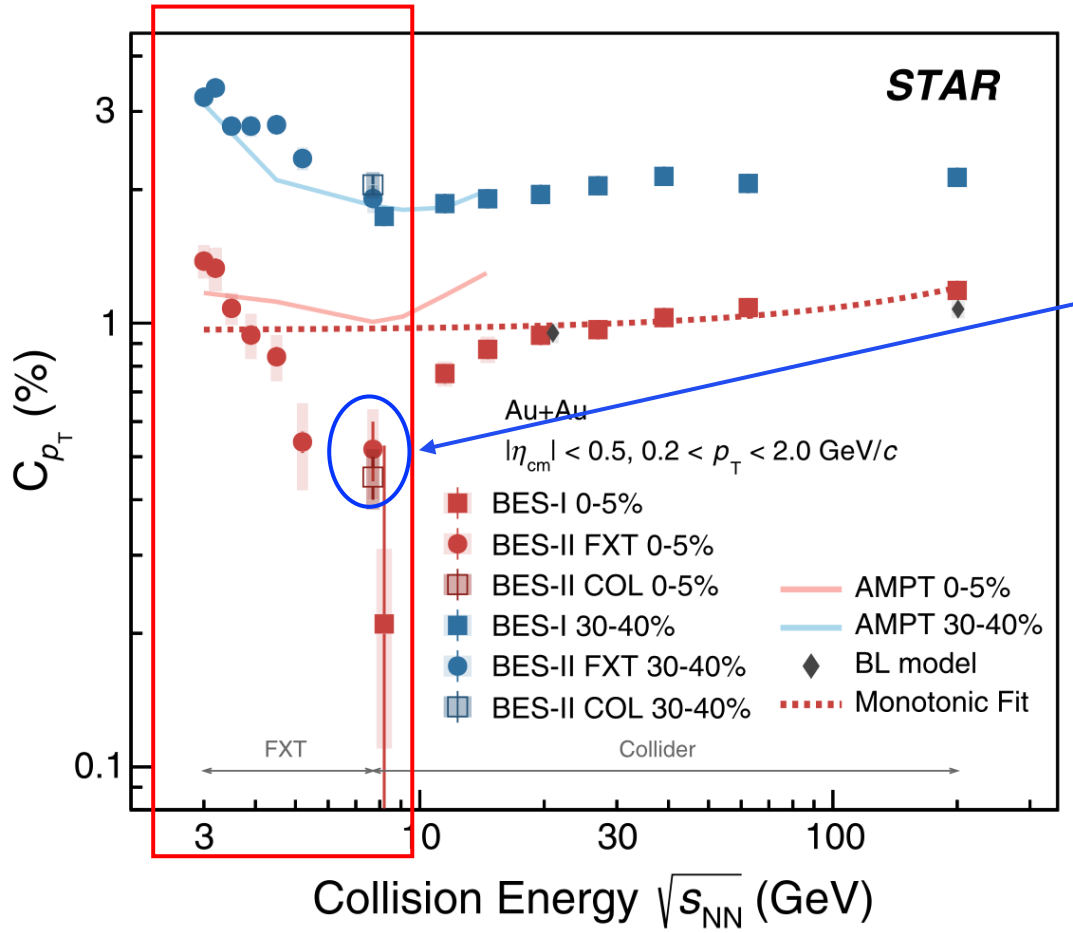
Nonmonotonicity of $\sqrt{\langle(\delta p_T)^2\rangle}/\langle\langle p_T\rangle\rangle$ vs collision energy in FXT mode

μ_B ~ 400 - 600 MeV

STAR, *PRL 137, 132301 (2026)*

BES-II results show a **significant non-monotonic behavior** in 0–5% central collisions, but not in 30–40%.

STAR 0-5 %	~5.5 σ
AMPT 0-5 %	~1.4 σ
STAR 30-40 %	~2 σ



No acceptance effect: at 7.7 GeV, BES-II is consistent with BES-I.

Useful for constraining EoS and understanding the phase diagram.

Ongoing: PID (pion/kaon/proton) STAR

Boltzmann–Langevin model: S. Gavin et. al., *PRC 95, 064901 (2017)*

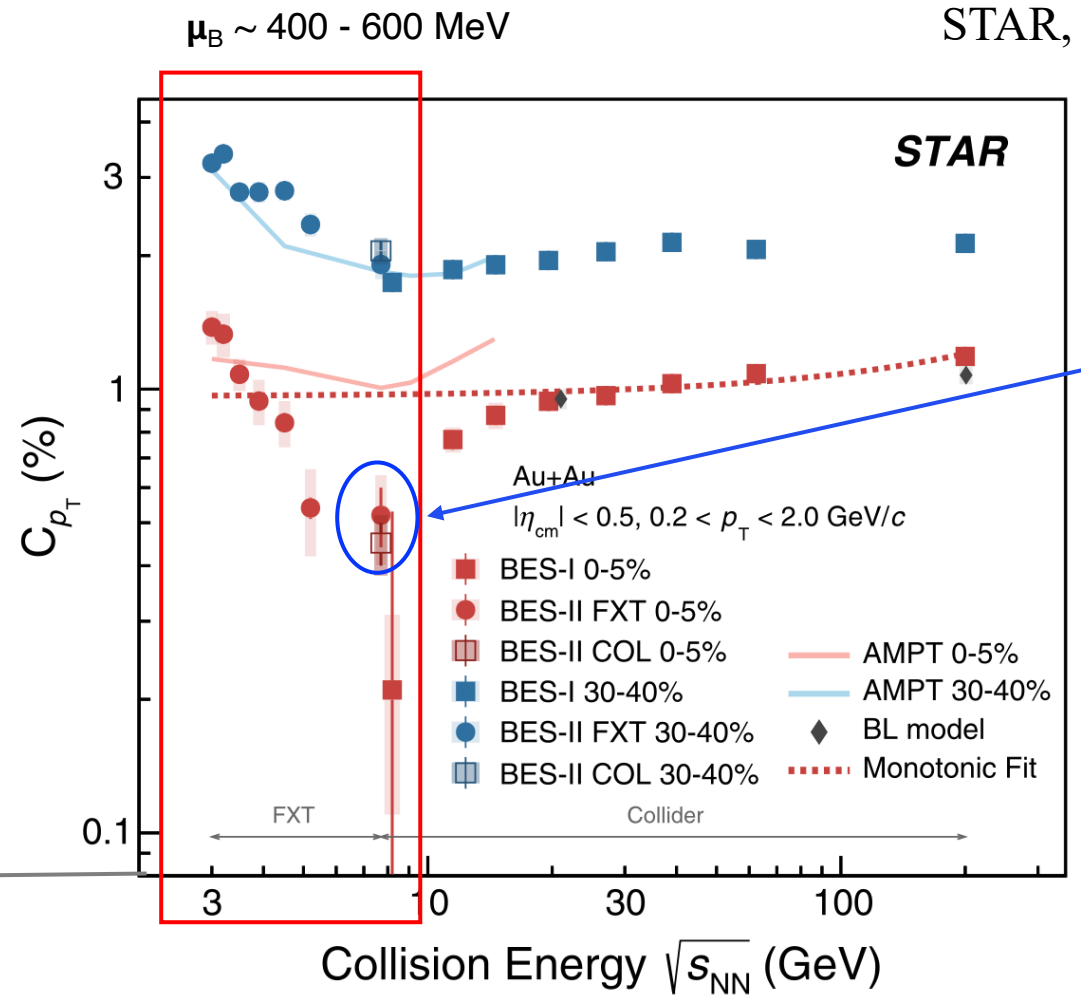
AMPT: L. Zhang, J. Chen, C. Zhang, *PRC 111, 024911 (2025)*; R.X. Cao, S. Zhang, Y.-G. Ma, *PRC 106, 014910 (2022)*

Nonmonotonicity of $\sqrt{\langle(\delta p_T)^2\rangle}/\langle\langle p_T\rangle\rangle$ vs collision energy in FXT mode

STAR, *PRL 137, 132301 (2026)*

BES-II results show a **significant non-monotonic behavior** in 0–5% central collisions, but not in 30–40%.

STAR 0-5 %	~5.5 σ
AMPT 0-5 %	~1.4 σ
STAR 30-40 %	~2 σ



No acceptance effect: at 7.7 GeV, BES-II is consistent with BES-I.

Lower-energy reaction measurable:

Nuclear liquid-gas phase transition region

100 MeV — 1 GeV

Y.-G. Ma, *PRL 83, 3617 (1999)*

Useful for constraining EoS and understanding the phase diagram.

Ongoing: PID (pion/kaon/proton) STAR

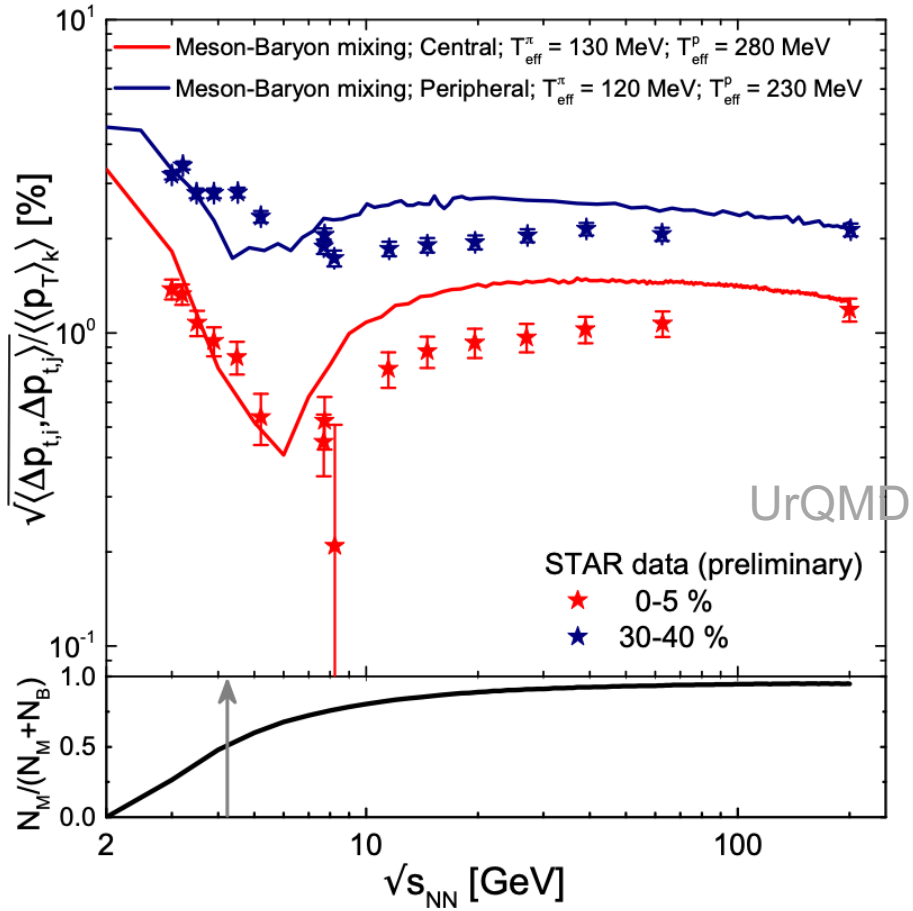
Boltzmann–Langevin model: S. Gavin et. al., *PRC 95, 064901 (2017)*

AMPT: L. Zhang, J. Chen, C. Zhang, *PRC 111, 024911 (2025)*; R.X. Cao, S. Zhang, Y.-G. Ma, *PRC 106, 014910 (2022)*

Interpretations: Baryon–Meson Composition

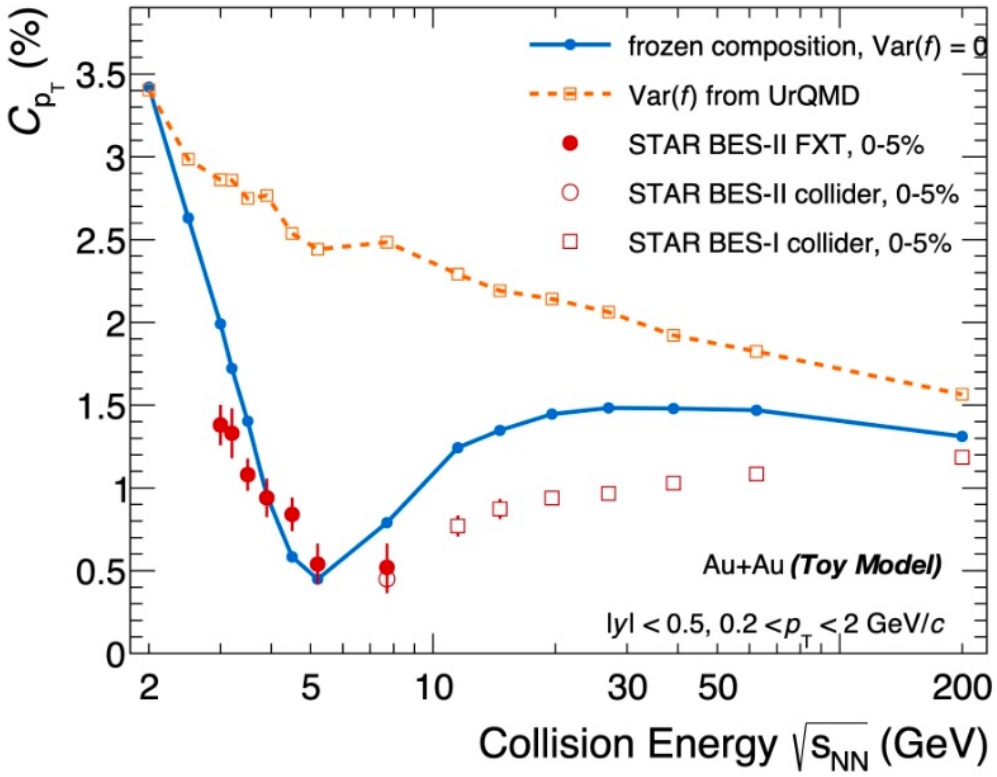
$$\langle \Delta p_{\mathrm{T},i} \Delta p_{\mathrm{T},j} \rangle = -\frac{N_M N_B}{N_k^2 (N_k - 1)} (\mu_M - \mu_B)^2$$

T. Reicherte, J. Steinheimera,b, M. Bleicher, *2606.03294*



Baryon–meson mixing can reproduce the observed non-monotonic energy dependence.

R. Manikandhan, R. Bellwied, *2610.32790.*

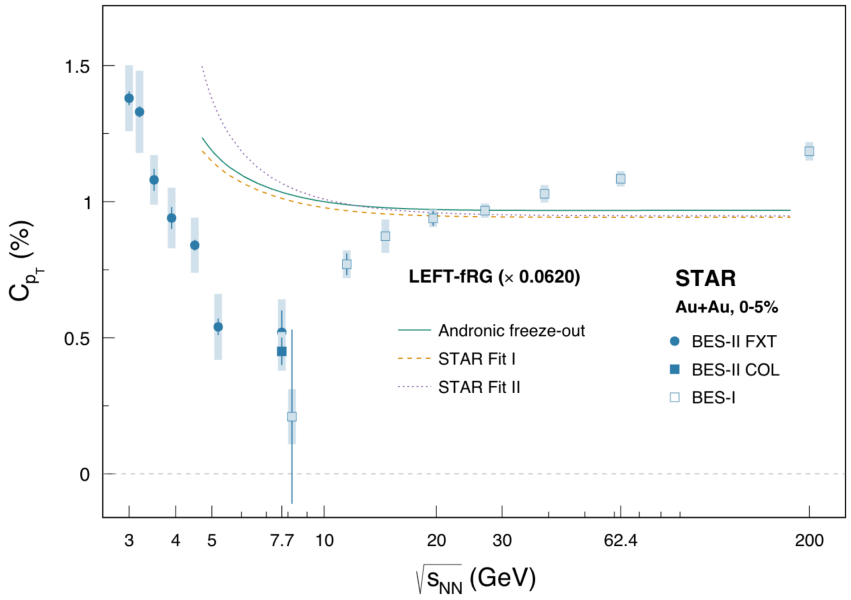


Including event-by-event composition fluctuations can wash out the dip.

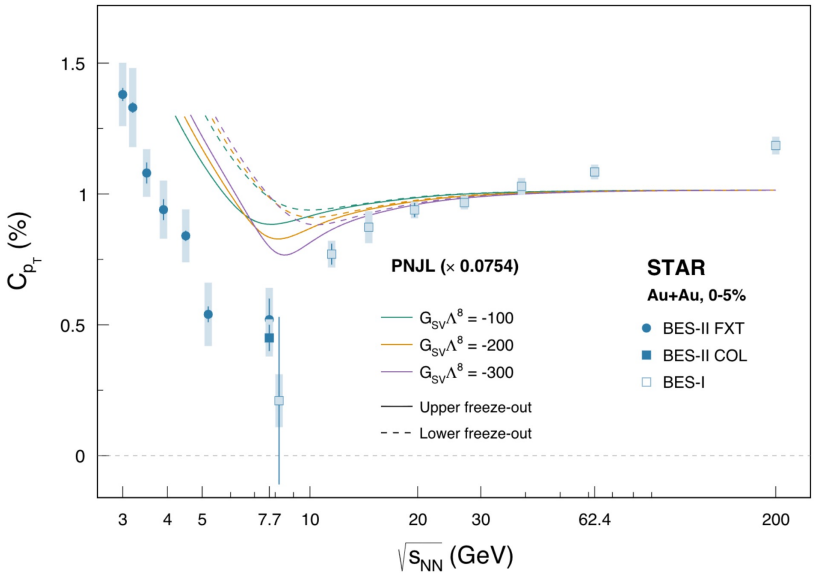
The non-monotonicity is sensitive not only to the mean baryon–meson composition, but also to its event-by-event fluctuations

Interpretations: Temperature fluctuations

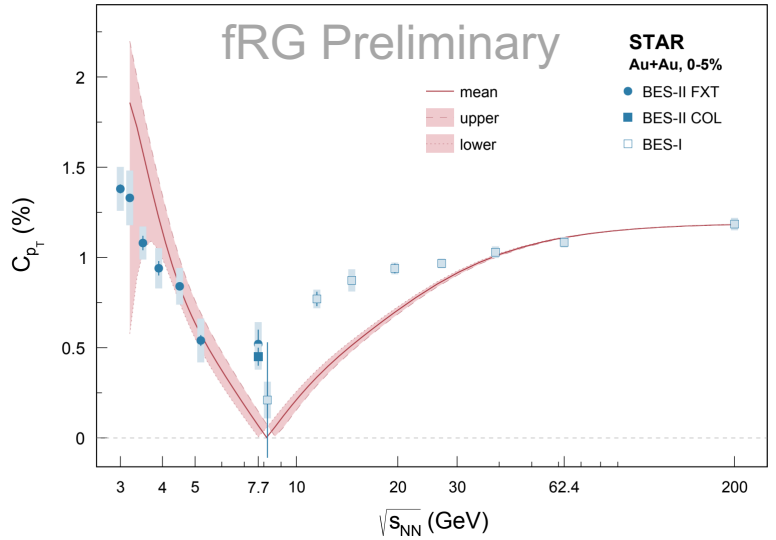
J. Chen, W. Fu, S. Yin, C. Zhang, *PRD 114, 014064 (2026)*



H. Liu, P. Wu, H.M. Liu, P.C. Chu, *2607.16275*



Y. Lu, F. Gao, J. M. Pawlowski, C. Zhang



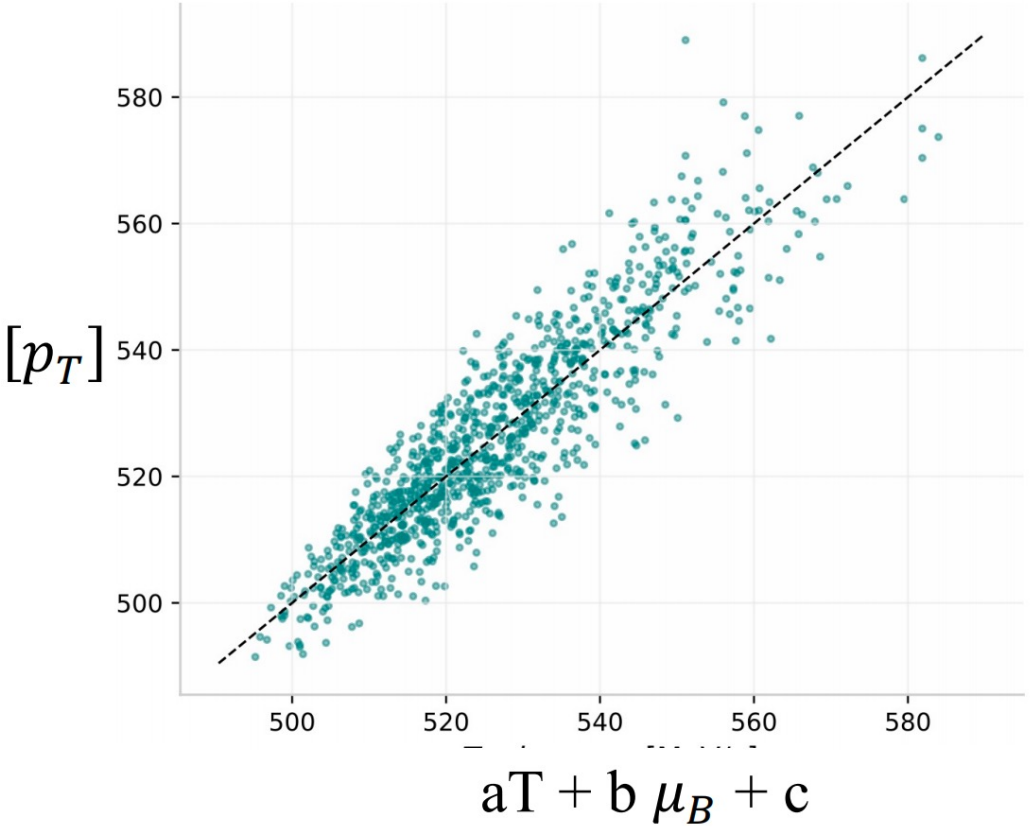
Reflecting their sensitivity to the QCD equation of state and freeze-out conditions

If the event-wise mean transverse momentum tracks the effective temperature, temperature fluctuations may contribute to the observed dynamical p_T correlations

Requires full dynamical modeling

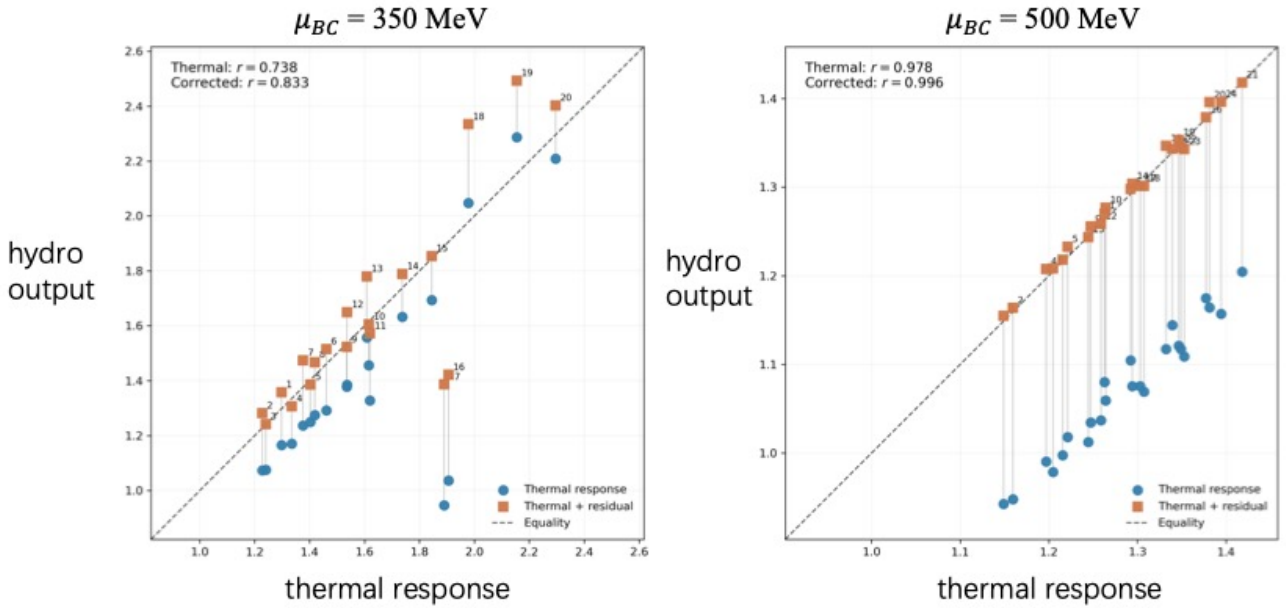
Interpretations: Hydrodynamic calculations

Hydrodynamic + EOS



Yushan Mu, C3NT, Searching for the QCD critical end point through fluctuations of intensive quantities

Numerical test of the thermal response in HIC: c_{p_T}



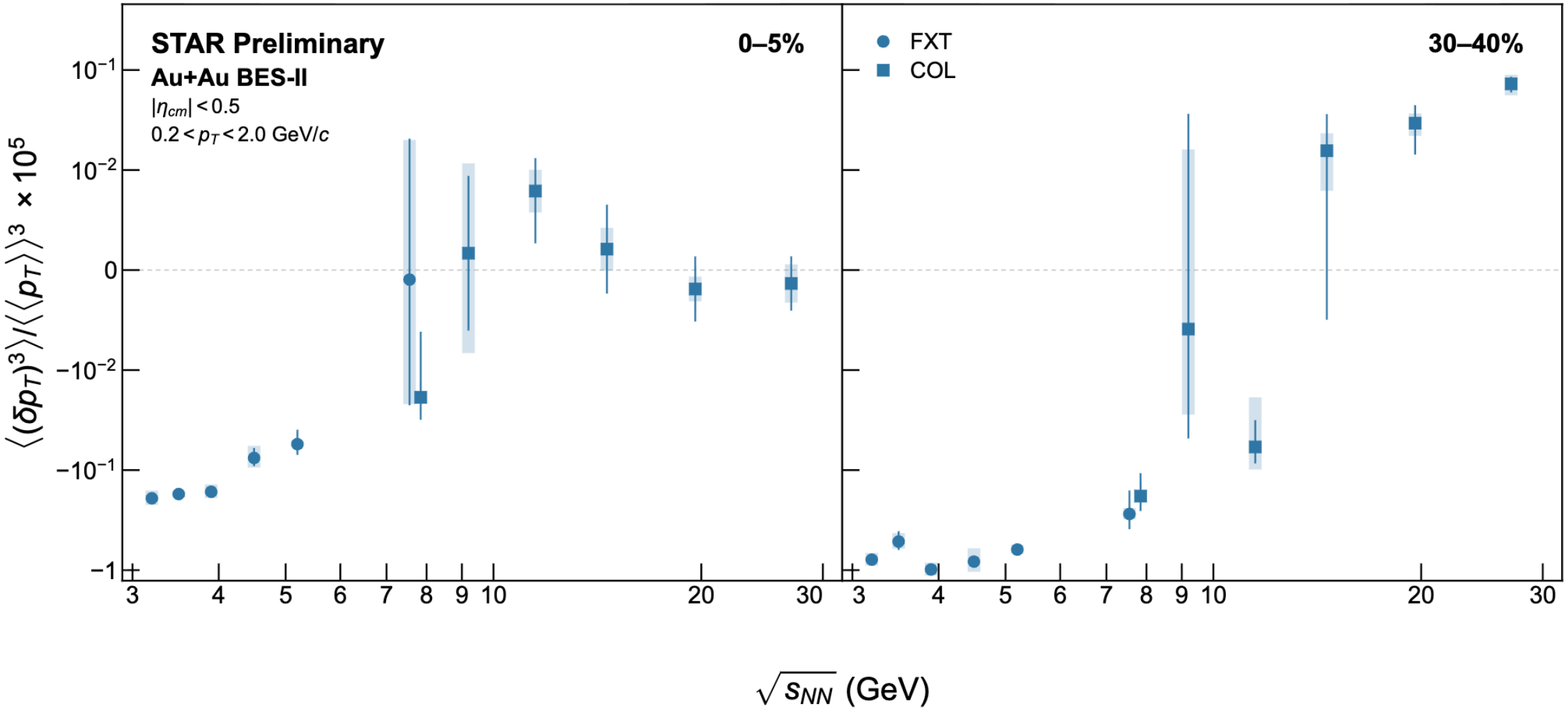
Fluctuations of $[p_T]$ is a sensitive probe of QCD EoS

Carry out event-by-event hydro simulations at finite muB with EoS embedded with CEP.

Require more theoretical understandings and calculations

II. Energy dependence of high-order p_T fluctuations

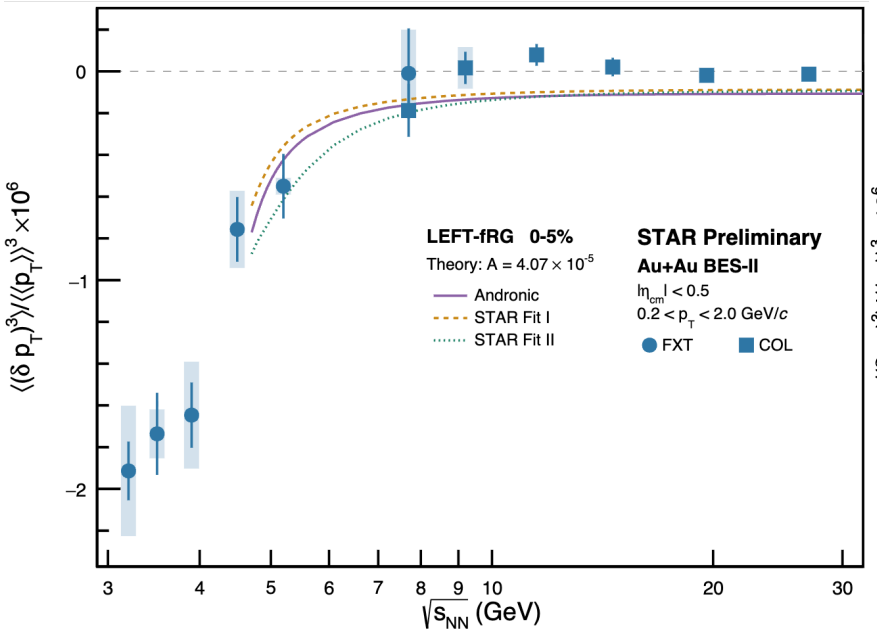
High-order $\langle(\delta p_T)^3\rangle/\langle p_T\rangle^3$ vs Energy



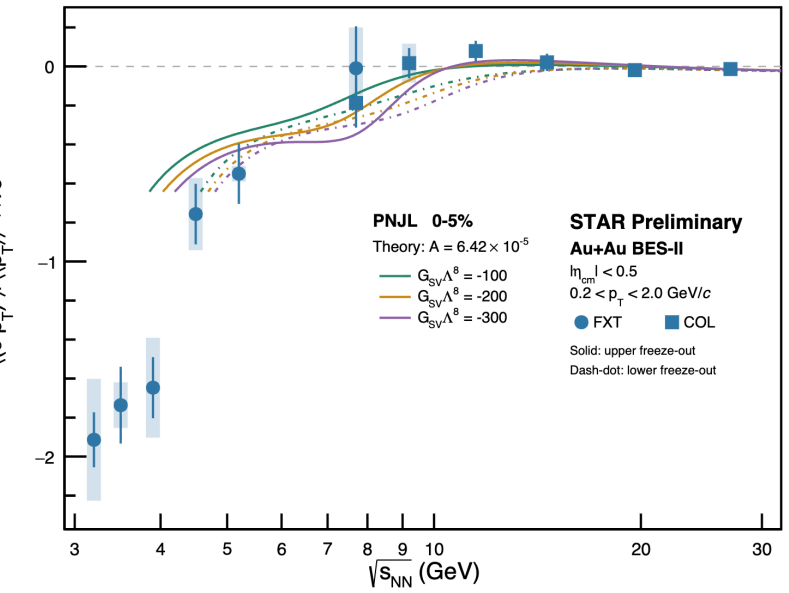
A pronounced negative-to-positive evolution is observed in 30–40% collisions, in contrast to the near-zero correlations at higher energies in 0–5%

Interpretations: Temperature fluctuations

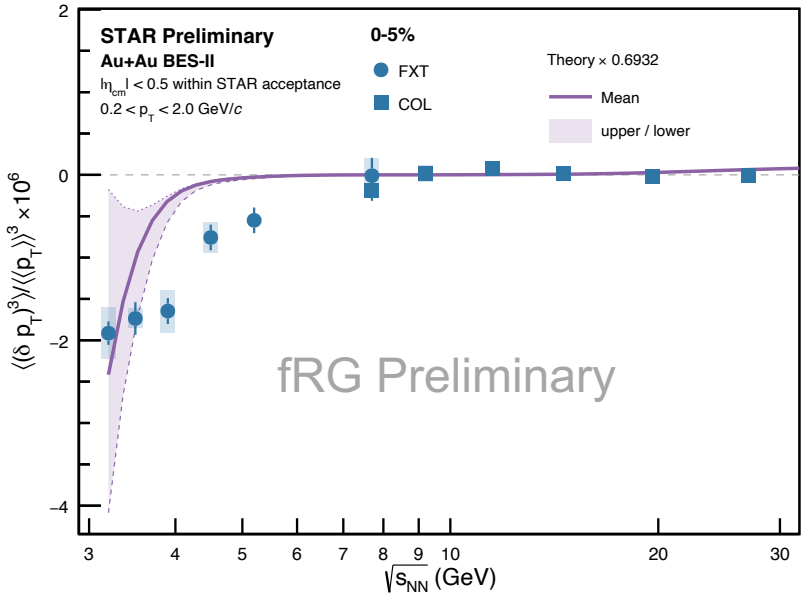
J. Chen, W. Fu, S. Yin, C. Zhang, PRD 114, 014064 (2026)



H. Liu, P. Wu, H.M. Liu, P.C. Chu, 2607.19275

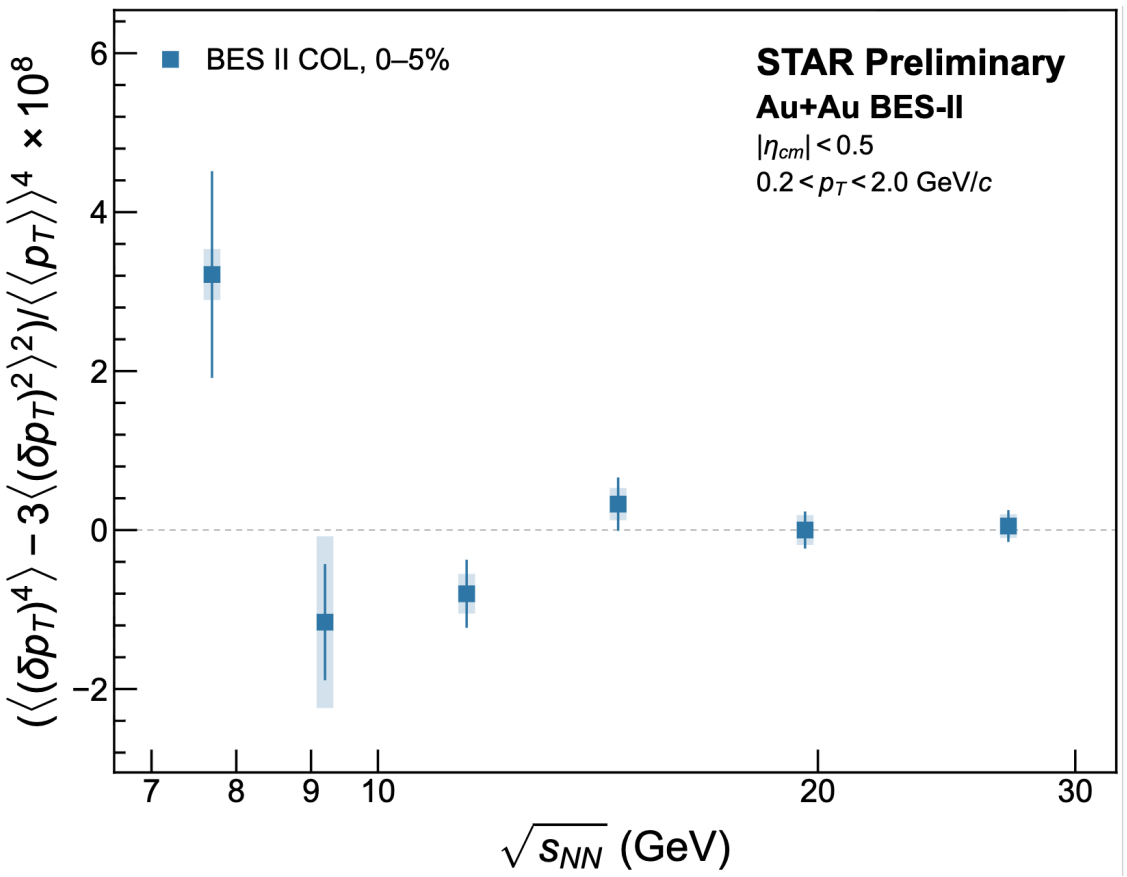


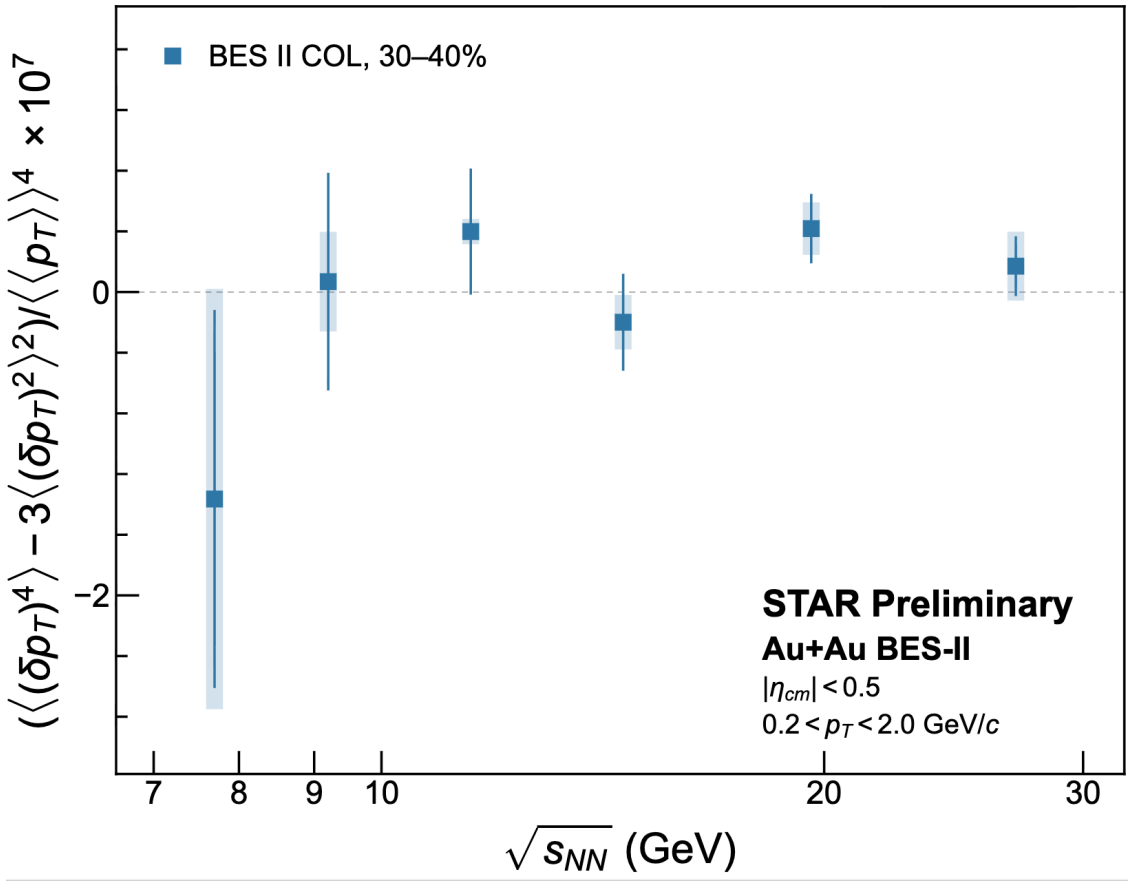
Y. Lu, F. Gao, J. M. Pawlowski, C. Zhang



- Both predict negative third-order temperature cumulants at low collision energies
- Qualitatively consistent with the overall trend of the STAR measurements
- Additional dynamical effects are useful for a comprehensive comparison in future

High-order $(\langle(\delta p_T)^4\rangle - 3\langle(\delta p_T)^2\rangle^2)/\langle p_T\rangle^3$ vs Energy

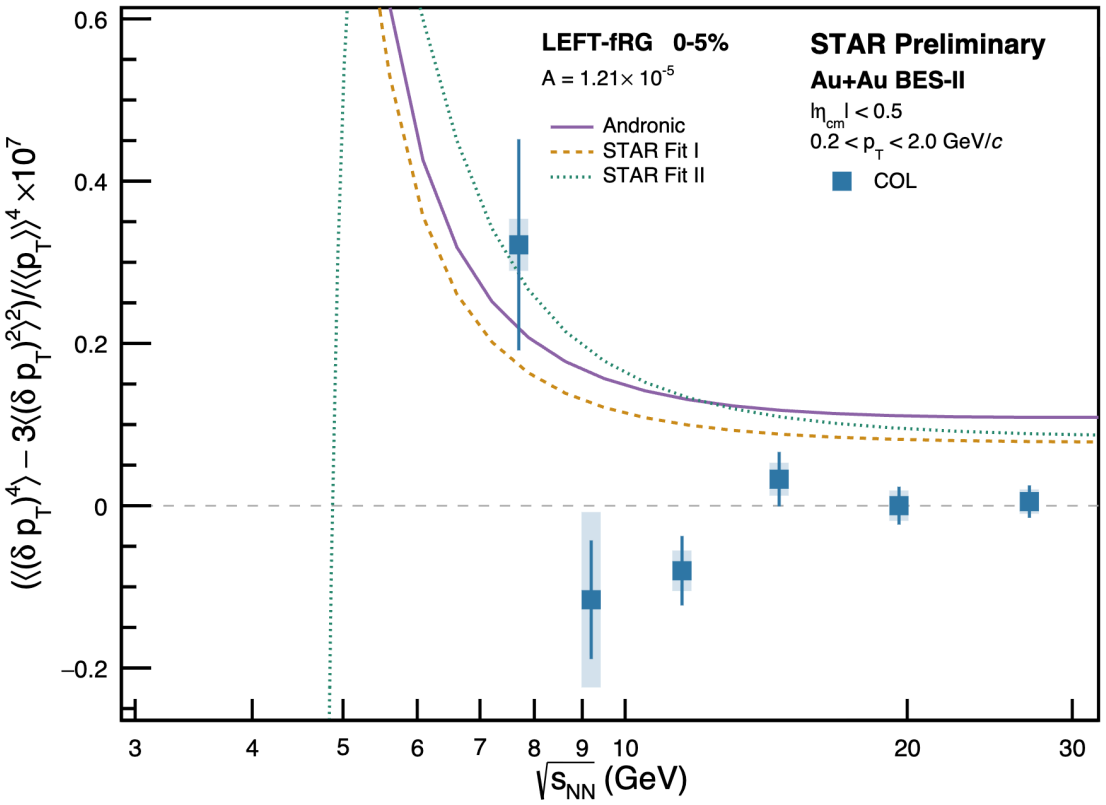




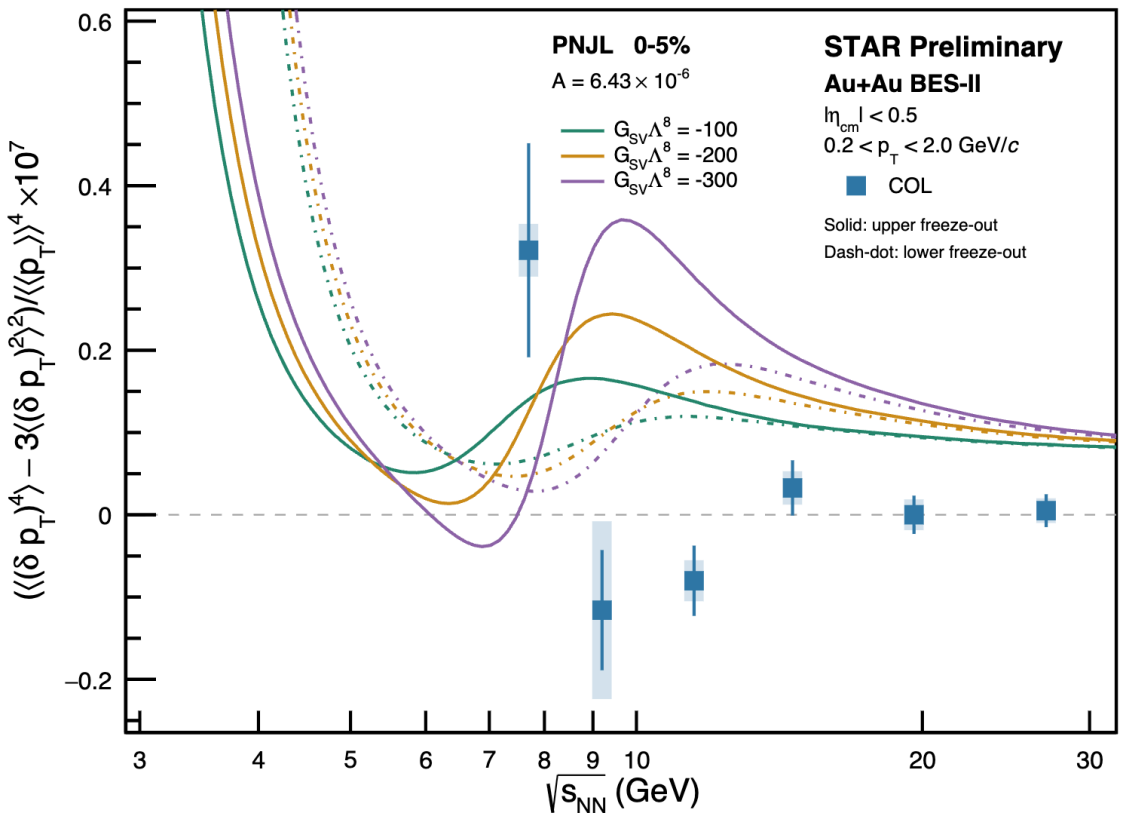
- 0–5%: Possible enhancement at low collision energies, with fourth-order cumulants approaching zero at higher energies
- 30–40%: Larger fourth-order correlations, fluctuating around zero

Interpretations: Temperature fluctuations

J. Chen, W. Fu, S. Yin, C. Zhang, PRD 114, 014064 (2026)



H. Liu, P. Wu, H.M. Liu, P.C. Chu, 2607.19275

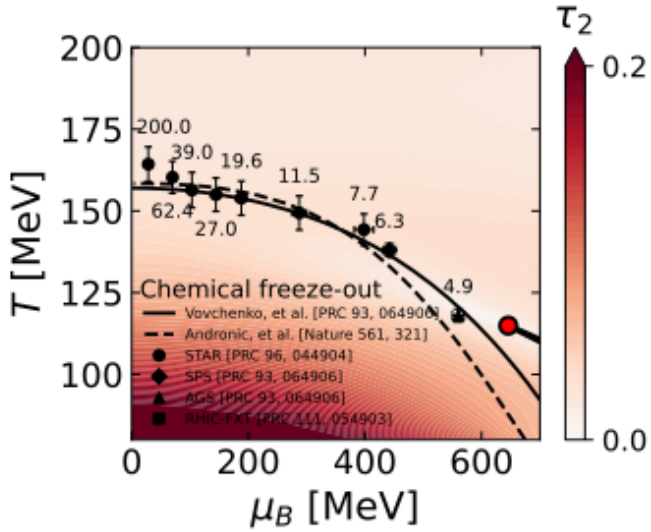


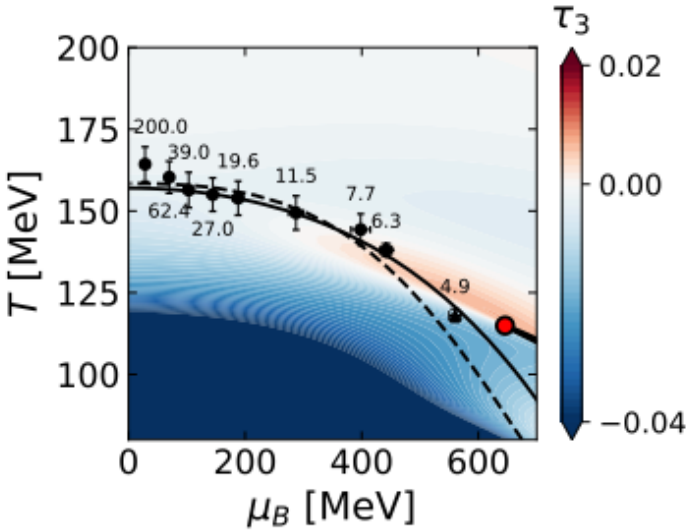
- LEFT-fRG: Positive fourth-order temperature cumulants, with a strong enhancement toward lower collision energies
- PNJL: Predicts non-monotonic peak–dip structures, sensitive to model parameters and freeze-out conditions

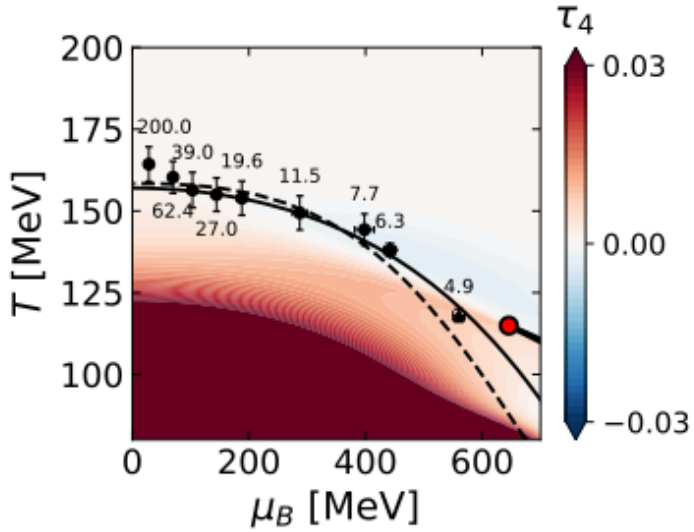
Qualitatively comparable with the overall trend of the STAR measurements

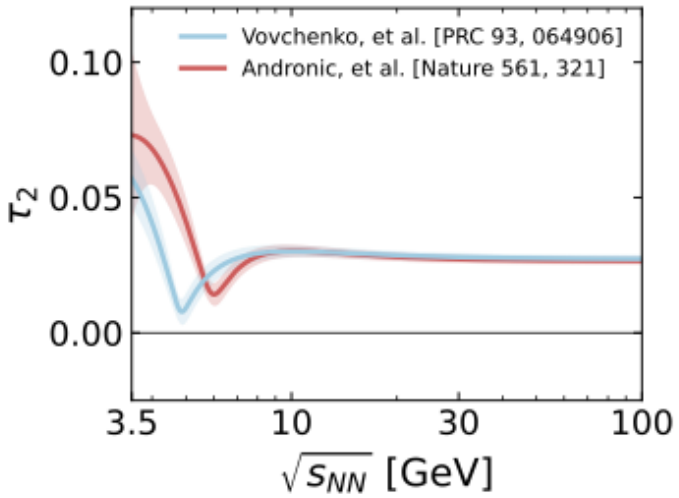
Interpretations: Temperature fluctuations

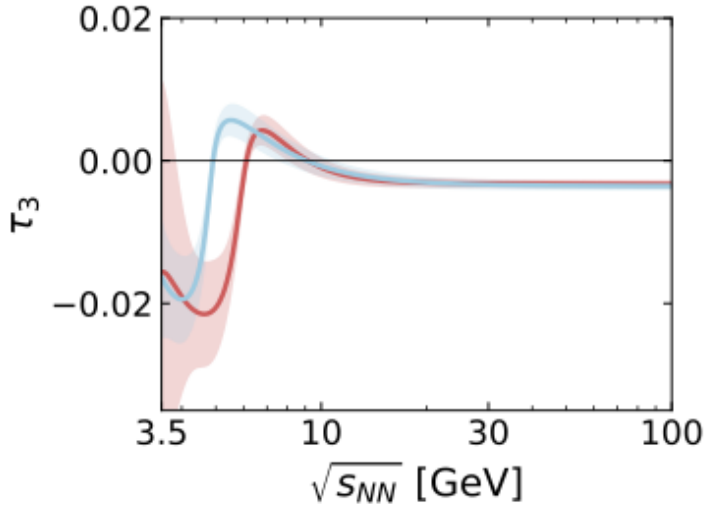
T. Gyure, H. Shah, L. Formaggio, F. D. Clemente, M. Hippert ,C. Ratti, V. Vovchenko, 2610.20806

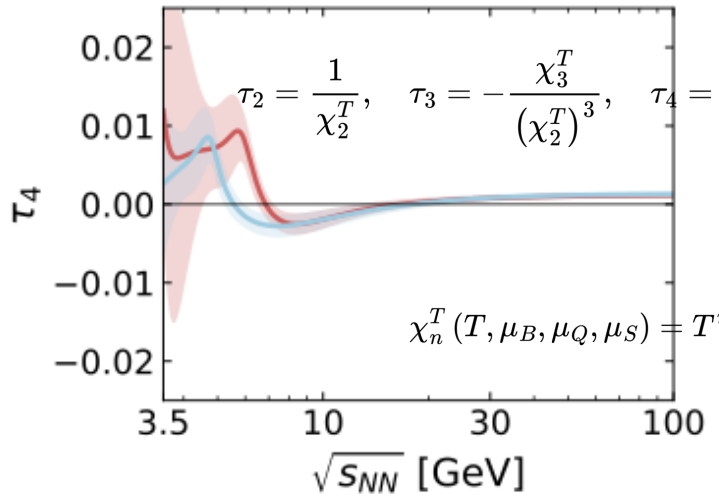












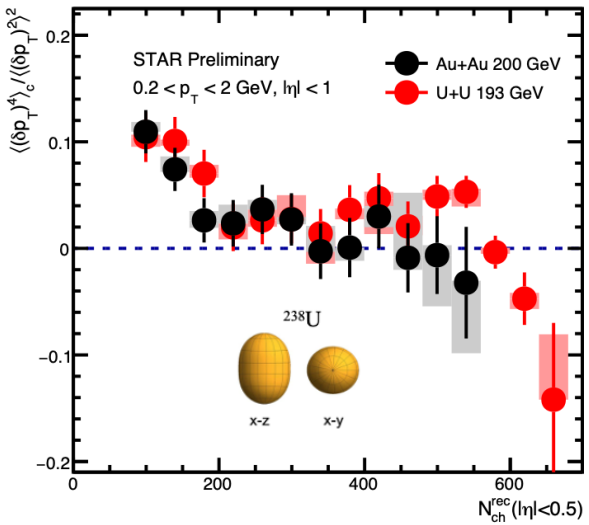
$$\tau_2 = \frac{1}{\chi_2^T}, \quad \tau_3 = -\frac{\chi_3^T}{(\chi_2^T)^3}, \quad \tau_4 = \frac{3(\chi_3^T)^2}{(\chi_2^T)^5} - \frac{\chi_4^T}{(\chi_2^T)^4}$$

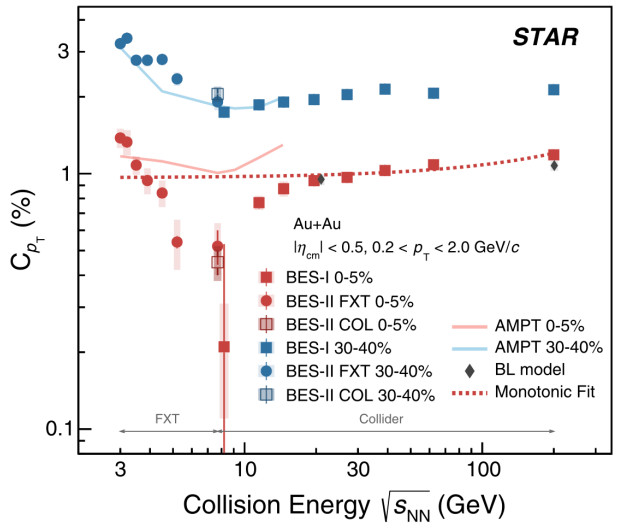
$$\chi_n^T(T, \mu_B, \mu_Q, \mu_S) = T^{n-4}\left(\frac{\partial^n p}{\partial T^n}\right)_{\mu_B, \mu_Q, \mu_S}$$

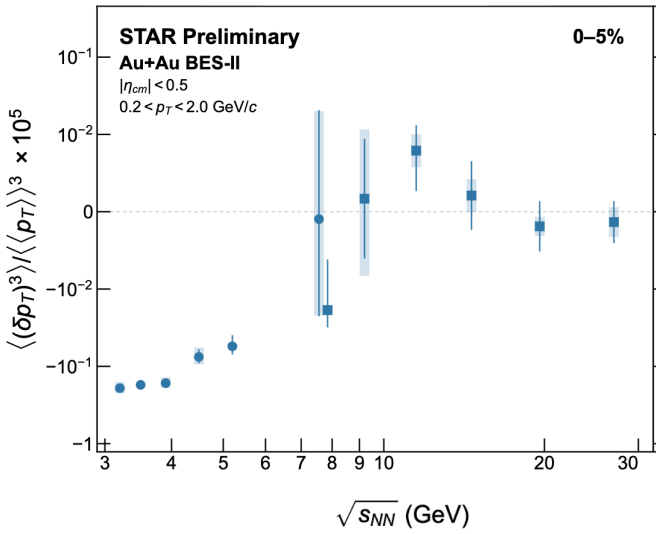
help distinguish critical behavior from a non-critical hadronic baseline around freeze-out lines approach the critical region of our equation of state.

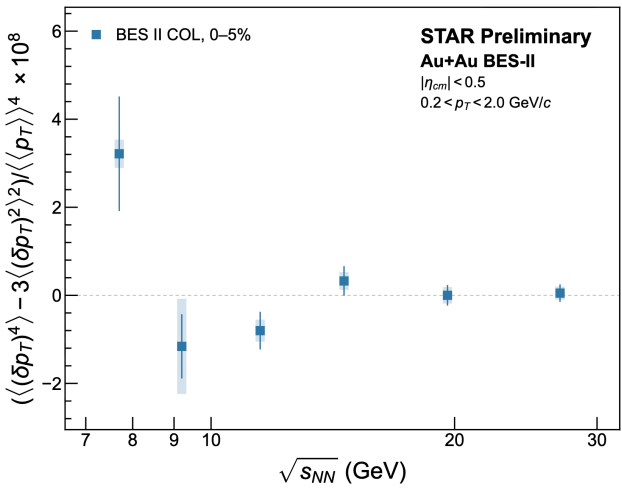
Conclusions

- **Mean p_T fluctuations: a potential smoking gun probing nuclear structure and QCD properties.**
- **Negative kurtosis** in highly deformed ^{238}U indicates the nuclear structure effect.
- Light ion collisions is a good connection to investigate **NN correlations and subnucleon fluctuations**.
- **Nonmonotonic dependence** of second-order mean p_T fluctuations at high μ_B.
- **High-order mean p_T fluctuations** serve as complementary probes of the properties of QCD matter.





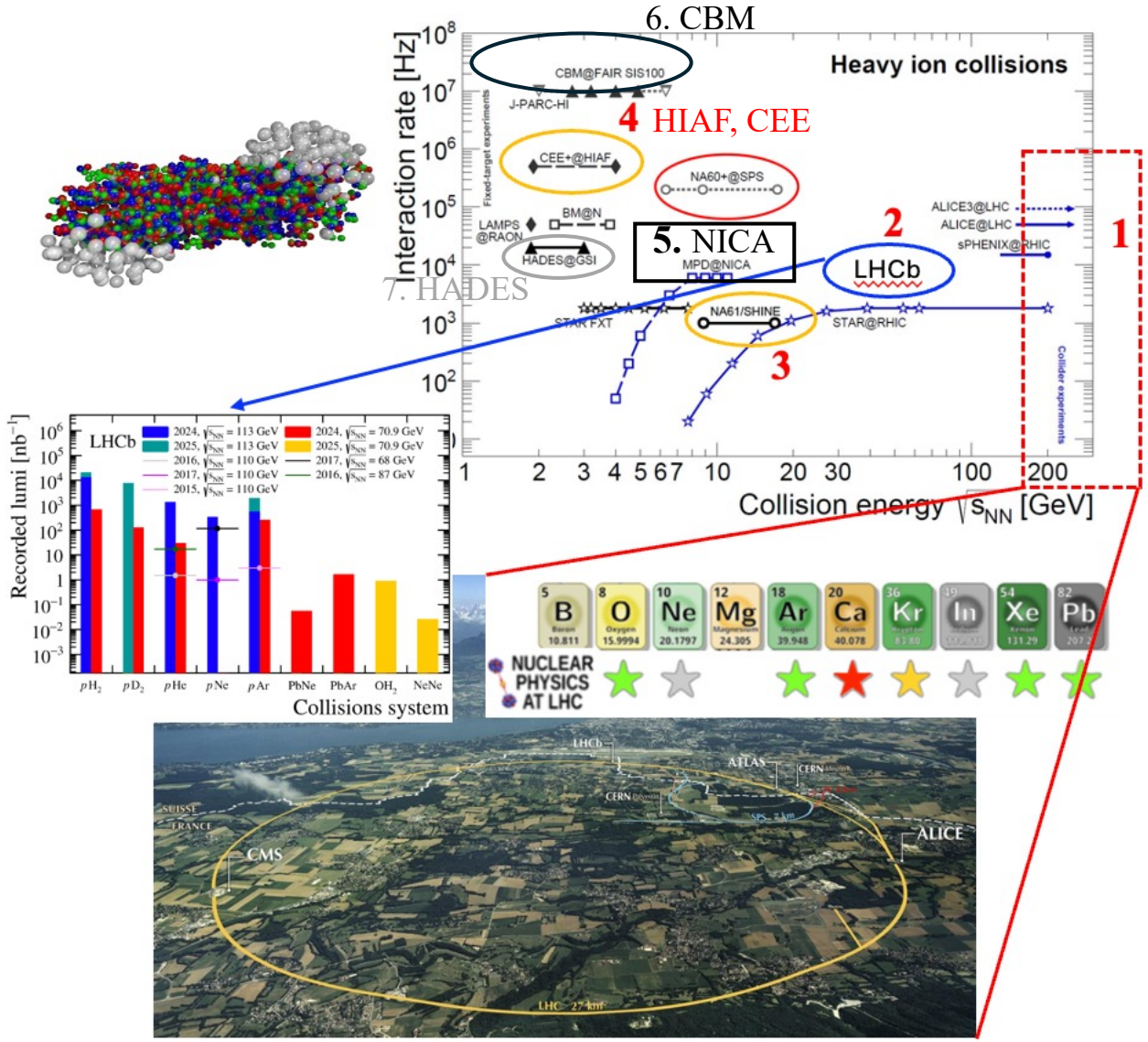




STAR, *PRL 137, 132301 (2026)*

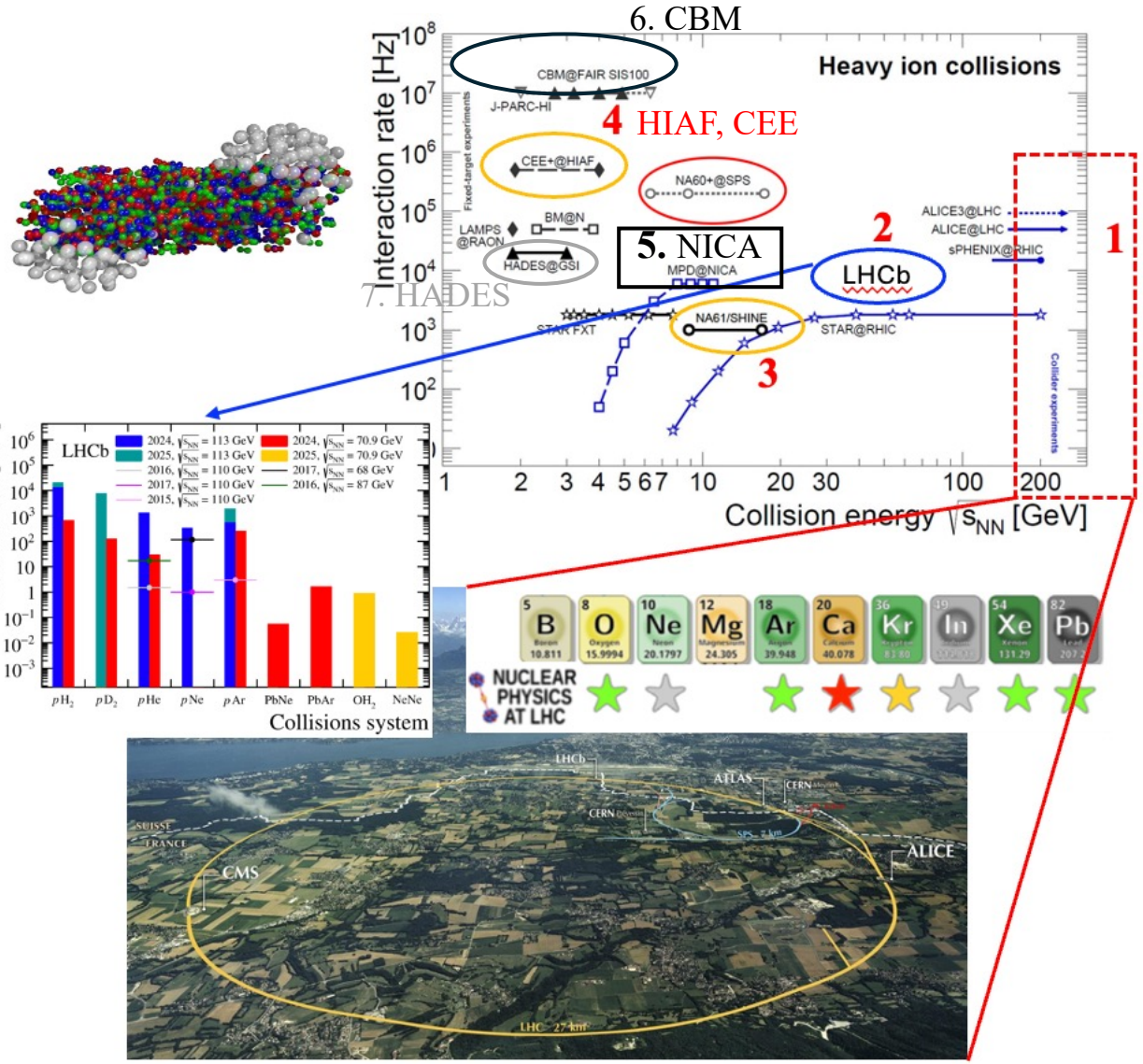
Outlooks

1) Energy evolution and system scan in high baryon density

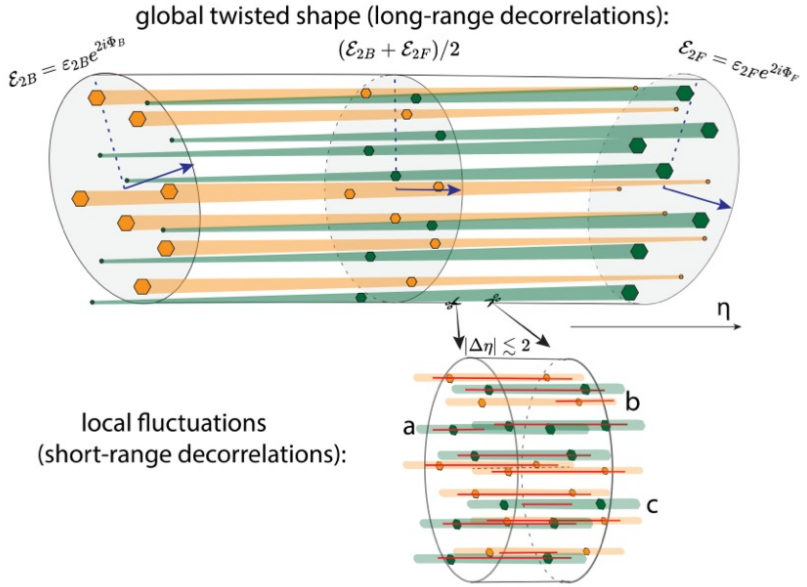


Outlooks

1) Energy evolution and system scan in high baryon density



2) Longitudinal structure QGP initial conditions



Decorrelation map:

v_n decorrelations (deformation-induced component):

C. Zhang, S. Huang, J. Jia, *2405.08749*

J. Jia, S. Huang, C. Zhang, S. Bhatta, *PRL 137, 202301 (2026)*

p_T decorrelations and EoS:

L. Liu, J. Chen, X.-G. Huang, J. Jia, C. Shen, C. Zhang, *2511.11094*

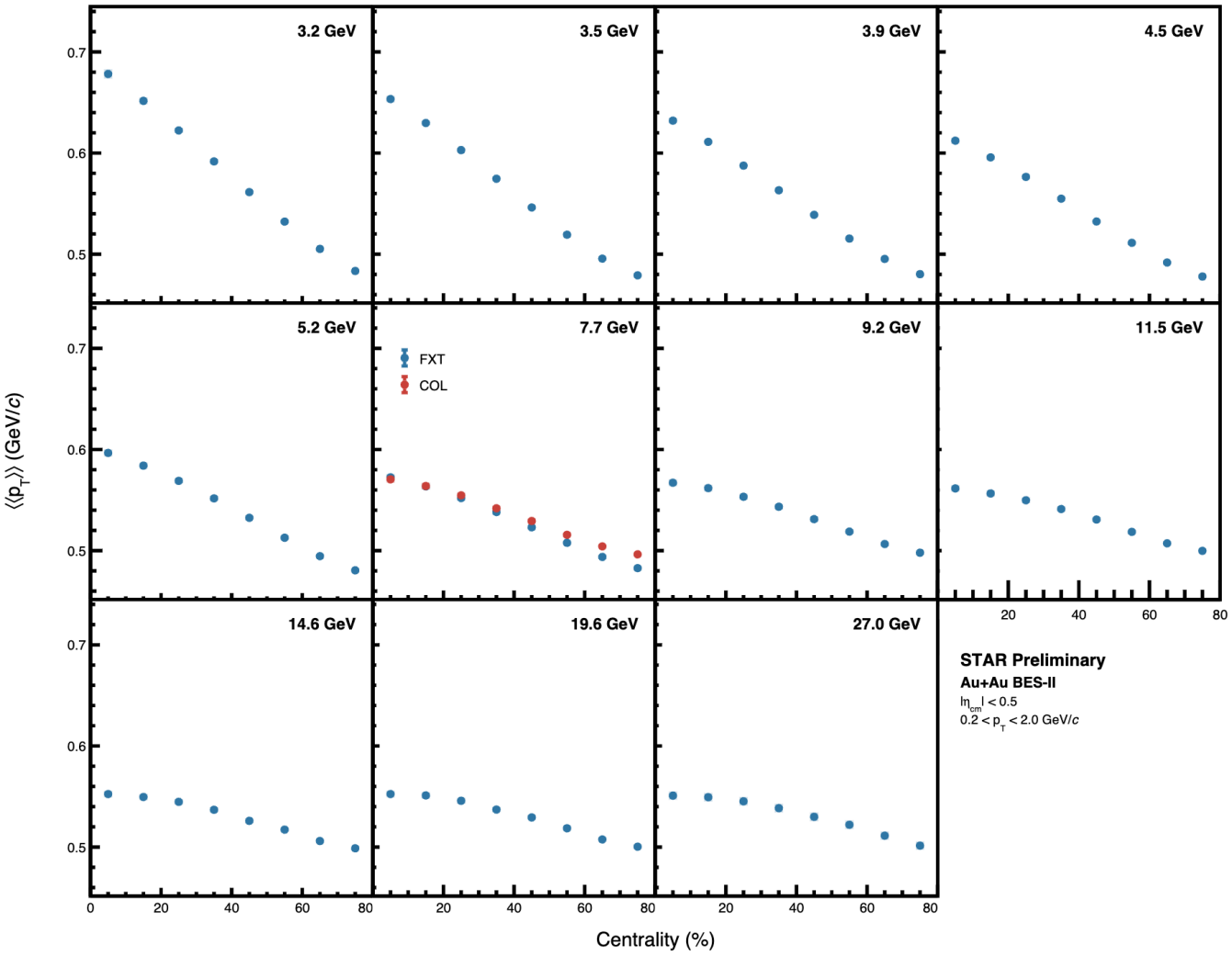
J. Zhu, X.-Y. Wu, G.-Y. Qin, *2602.04148*

S. Jahan, Roch, C. Shen, *PRC 113, 024919 (2026)*

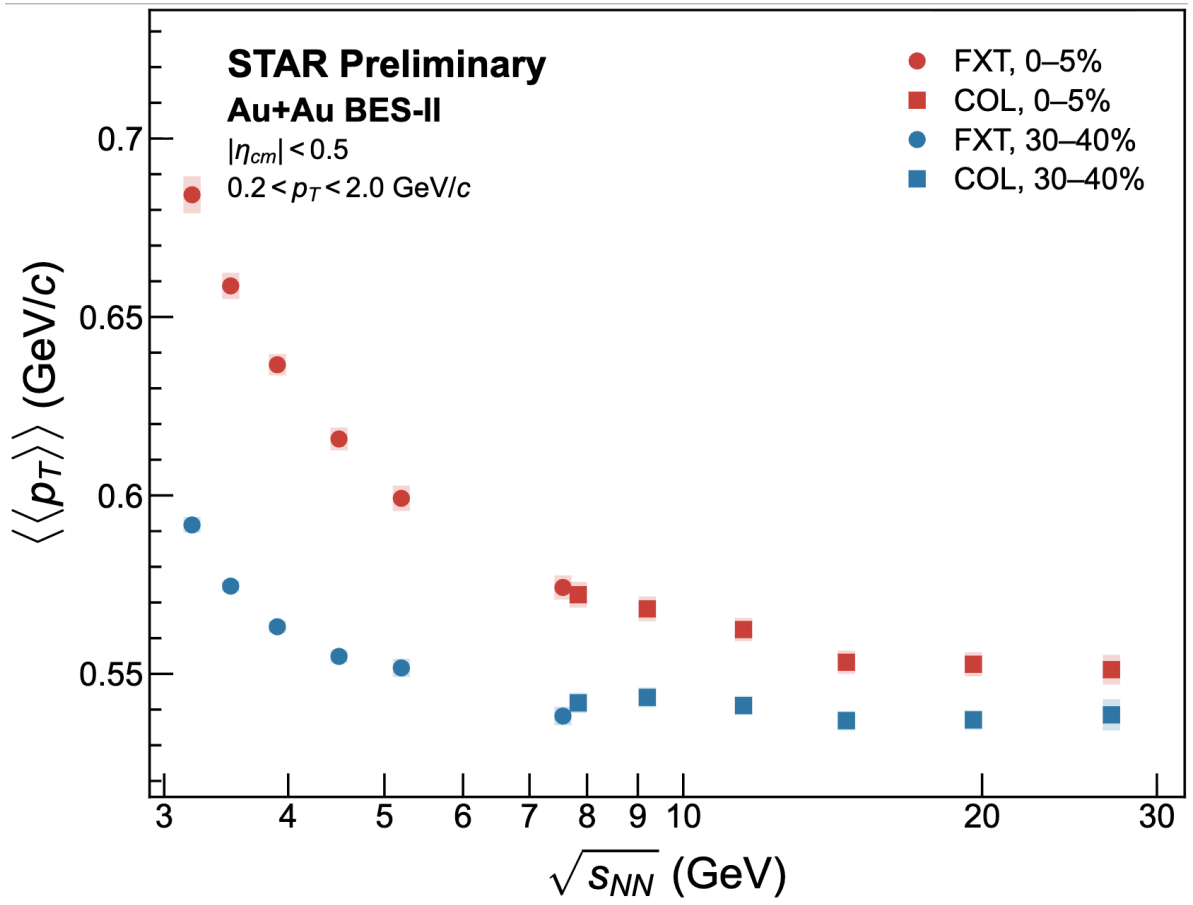
...

Thank you for your attention!

Centrality and Energy dependence of $\langle p_T \rangle$



Stronger Centrality dependence at lower energies.



Mean p_T decreases rapidly at low collision energies and shows a much weaker variation above 11.5 GeV